THE JOURNAL OF BIOLOGICAL CHEMISTRY VOL. 287, NO. 42, pp. 35669–35677, October 12, 2012

Induction of Cardiac Fibrosis by β-Blocker in G Protein-independent and G Protein-coupled Receptor Kinase 5/β-Arrestin2-dependent Signaling Pathways*[S]

Received for publication, February 29, 2012, and in revised form, July 19, 2012 Published, JBC Papers in Press, August 10, 2012, DOI 10.1074/jbc.M112.357871

Michio Nakaya[‡], Satsuki Chikura[‡], Kenji Watari[‡], Natsumi Mizuno[‡], Koji Mochinaga[‡], Supachoke Mangmool[‡], Satoru Koyanagi[§], Shigehiro Ohdo[§], Yoji Sato[¶], Tomomi Ide[‖], Motohiro Nishida[‡], and Hitoshi Kurose[‡1]

From the Departments of [‡]Pharmacology and Toxicology and [§]Pharmaceutical Sciences, Graduate School of Pharmaceutical Sciences, and the [‖]Department of Cardiovascular Medicine, Graduate School of Medical Sciences, Kyushu University, Fukuoka 812-8582 and the [¶]Division of Cellular and Gene Therapy Products, National Institute of Health Sciences, Setagaya, Tokyo 158-8501, Japan

Background: It is not known whether a β-blocker, metoprolol, induces physiological responses through β-arrestins *in vivo*.
Results: Long-term administration of metoprolol induced cardiac fibrosis in wild type but not β-arrestin2- or GRK5 knock-out mice.
Conclusion: Metoprolol induced cardiac fibrosis in a G protein-independent and GRK5/β-arrestin2-dependent manner.
Significance: Our study provides a physiological significance of β-arrestin-mediated biased signaling pathway by a β-blocker *in vivo*.

G-protein coupled receptors (GPCRs) have long been known as receptors that activate G protein-dependent cellular signaling pathways. In addition to the G protein-dependent pathways, recent reports have revealed that several ligands called "biased ligands" elicit G protein-independent and β-arrestin-dependent signaling through GPCRs (biased agonism). Several β-blockers are known as biased ligands. All β-blockers inhibit the binding of agonists to the β-adrenergic receptors. In addition to β-blocking action, some β-blockers are reported to induce cellular responses through G protein-independent and β-arrestin-dependent signaling pathways. However, the physiological significance induced by the β-arrestin-dependent pathway remains much to be clarified *in vivo*. Here, we demonstrate that metoprolol, a β_1-adrenergic receptor-selective blocker, could induce cardiac fibrosis through a G protein-independent and β-arrestin2-dependent pathway. Metoprolol, a β-blocker, increased the expression of fibrotic genes responsible for cardiac fibrosis in cardiomyocytes. Furthermore, metoprolol induced the interaction between β_1-adrenergic receptor and β-arrestin2, but not β-arrestin1. The interaction between β_1-adrenergic receptor and β-arrestin2 by metoprolol was impaired in the G protein-coupled receptor kinase 5 (GRK5)-knockdown cells. Metoprolol-induced cardiac fibrosis led to cardiac dysfunction. However, the metoprolol-induced fibrosis and cardiac dysfunction were not evoked in β-arrestin2- or GRK5-knock-out mice. Thus, metoprolol is a biased ligand that selectively activates a G protein-independent and GRK5/β-arrestin2-dependent pathway, and induces cardiac fibrosis. This study demonstrates the physiological importance of biased agonism, and suggests that G protein-independent and β-arrestin-dependent signaling is a reason for the diversity of the effectiveness of β-blockers.

G protein-coupled receptors (GPCRs)[2] mediate physiological responses to a variety of ligands, such as hormones, neurotransmitters, and environmental stimuli, and are tightly regulated by several mechanisms (1). Among the mechanisms, GPCR kinase (GRK) and β-arrestin-mediated events are known as general mechanisms of GPCR functional regulation (2–6). When an agonist binds to GPCR, it activates a cellular signal transduction cascade through G proteins, but also induces GRK/β-arrestin-mediated events to prevent excess stimulation. GRKs phosphorylate the agonist-bound GPCRs, and β-arrestins bind to the phosphorylated receptors, and then inhibit further stimulation of G proteins by the agonist-bound receptors through steric hinderance. As β-arrestins can also bind clathrin and adaptor proteins, the phosphorylated and β-arrestin-bound receptors are internalized into endocytic vesicles (7). The internalized receptors then are recycled back to the plasma membrane or directed to the degradation pathway by undefined processes (8, 9). In addition to the receptor regulation, it has been recently recognized that GRKs and β-arrestins mediate cellular signaling by GPCRs independently of G protein activation (2–4, 10, 11). However, these GRK- and β-arrestin-dependent signaling pathways are largely demonstrated by *in vitro* cellular systems. To establish the physiological impor-

* This work was supported by grants from the Ministry of Education, Culture, Sports, Science, and Technology of Japan (to M. Na, M. Ni, and H. K.), a Grant-in-aid for Scientific Research on Innovative Areas (to M. Ni), a Grant-in-aid for Scientific Research on Priority Areas (to H. K.), the Takeda Science Foundation and the Mochida Memorial Foundation for Medical and Pharmaceutical Research (to M. Na).
[S] This article contains supplemental Figs. S1–S4 and Movies S1 and S2.
[1] To whom correspondence should be addressed: Kyushu University, 3-1-1 Maidashi, Higashi-ku, Fukuoka 812-8582, Japan. Tel./Fax: 81-92-642-6884; E-mail: kurose@phar.kyushu-u.ac.jp.

[2] The abbreviations used are: GPCR, G protein-coupled receptor; GRK, G protein-coupled receptor kinase; BRET, bioluminescence resonance energy transfer; FRET, fluorescence resonance energy transfer; CTGF, connective tissue growth factor; Col1a, collagen 1α; Rluc, *Renilla* luciferase; KO, knockout.

tance of the signaling pathways, it is essential to demonstrate GRK- and β-arrestin-dependent responses *in vivo*.

β-Adrenergic receptors are members of the G protein-coupled receptor family and are pharmacologically and genetically subdivided into three subtypes: β_1, β_2, and β_3 (12). The β_1-adrenergic receptor is involved in the regulation of cardiac functions as well as in the induction and development of various cardiovascular diseases including heart failure (13, 14). During heart failure, a large amount of catecholamine is believed to be released from synaptic ends (15, 16), and exerts harmful effects on the heart. Therefore, administration of β-adrenergic receptor antagonists, β-blockers, is effective for patients in the early stages of heart failure (17). So far, various kinds of β-blockers have been developed, but many basic and clinical studies indicate that the effect of each β-blocker is divergent (18). Several reasons, including receptor selectivity, antioxidant property, and membrane-stabilizing effects have been proposed for the diversity, but there still remains much to be known. Understanding the reasons more properly would help to develop a more efficient β-blocker with fewer side effects.

In addition to the blocking effects, some β-blockers have been shown to evoke signal transduction through the β-adrenergic receptors in G protein-independent and β-arrestin-dependent manner (19–21). Like β-blockers, some agonists for seven-transmembrane receptors have been reported not only to transmit the classic G protein signaling, but also to generate the signaling in a G protein-independent fashion (22–25). These agonists and phenomena are called "biased ligands" and "biased agonism," respectively (11). To date, the signal transduction pathways by biased ligands have been intensively unveiled by *in vitro* studies. However, the physiological meaning of the biased ligand-mediated signaling is hardly clarified *in vivo*.

We found that long-term administration of metoprolol, an inverse agonist for the β_1-adrenergic receptor, to mice induced cardiac fibrosis, which is thought to be deleterious for the heart by stiffening it and inhibiting the electrical conductivity between cardiomyocytes. We revealed that this fibrotic pathway was mediated through the β_1-adrenergic receptor in a G protein-independent manner. We also discovered that β-arrestin2 and GRK5 are involved in this G protein-independent fibrotic pathway not only *in vitro* but also *in vivo*.

EXPERIMENTAL PROCEDURES

Animals and Administration of β-Blockers—We purchased ddY, C57BL/6J mice, and Sprague-Dawley rats from KYUDO (Japan). GRK5-, GRK6-, and β-arrestin2-KO mice were obtained by Drs. R. J. Lefkowitz and R. T. Premont (Duke University). Administration of β-blockers was started at 6 weeks of age of male mice. β-Blockers (metoprolol, 30 mg/kg/day; carvedilol, 30 mg/kg/day; propranolol, 10 mg/kg/day) or saline were orally administered twice a day for 3 months. All experiments using mice and rats were approved by the guidelines of Kyushu University.

Isolation of Cardiac Cells and Transfection—Rat neonatal cardiomyocytes and cardiac fibroblasts were isolated as described previously (26, 27). In brief, 1-day-old Sprague-Dawley rats are deeply anesthetized and their hearts were expeditiously extirpated on ice. The atria of the extirpated hearts are quickly removed by using sterilized forceps and scissors. The remaining hearts were cut into small pieces and digested by collagenase. The digested cells were plated on 10-cm plates for 1 h at 37 °C and nonattached cells or attached cells were used as cardiomyocytes or cardiac fibroblasts, respectively. The cardiomyocytes are plated on gelatin-coated 6-well plates (3×10^4 cells/well). When siRNAs were transfected into cardiomyocytes, Lipofectamine 2000 was used. Plasmid DNAs were transfected into the rat neonatal cardiomyocytes or H9c2 cells by electroporation and into HEK293 cells by FuGENE6 (Roche Applied Science).

BRET Assay—To evaluate the interaction between β_1-adrenergic receptor and β-arrestin2, or the conformational changes in β-arrestin2, BRET experiments were performed as described previously (28, 29). The plasmids of β_1-adrenergic receptor-*R*luc, GFP^2-β-arrestin1, and β-arrestin2-GFP^2 were transfected into HEK293 cells, H9c2 cells, or rat neonatal cardiomyocytes. *R*luc-β-arrestin2-GFP^2 was expressed in HEK293 or H9c2 cells. These cells stably expressed the β_1-adrenergic receptor. Forty-eight hours after the transfection, the cells were collected and washed by DMEM/F12 (Invitrogen). The cells were suspended in the assay buffer (0.1 g/liter of $CaCl_2$, 0.1 g/liter of $MgCl_2 \cdot 6H_2O$, 1 g/liter of D-glucose, and 2 μg/ml of aprotinin in PBS) to adjust 5×10^4 cells/ml. Then, 25 μl of the cell suspension was distributed in a 96-well white microplate and 25 μl of the drug solution was added. After a 5-min incubation, DeepBlueC™ was added at a final concentration of 5 μM and the 400 nm (*R*luc) and 515 nm (GFP^2) emissions were immediately measured using a Multilabel Reader Mithras LB 940 (Berthold Technologies).

FRET Assay—The FRET probe to monitor the changes of the concentration of cAMP was constructed as reported previously (30). HEK293 cells stably overexpressing the β_1-adrenergic receptor were plated on poly-L-lysine-coated 35-mm glass-bottom base dishes and transfected with the FRET probe. Two days after transfection, the culture medium was replaced by phenol red-free medium (DMEM/F-12) containing 0.1% fetal bovine serum, and more than 3 h later, the cells were imaged by the microscopy (Olympus IX-81) in a heated chamber kept at 37 °C. In some experiments of β-blocker stimulation, drugs other than β-blockers were added before the stimulation. ICI118551 (50 μM) or pertussis toxin (100 ng/ml) were added 10 min or 16 h before the stimulation of β-blockers, respectively. 3-Isobutyl-1-methylxanthine (1 mM) was added simultaneously with each β-blocker. The images for CFP, YFP, and DIC were taken every 1 min. Image analysis was performed by MetaMorph software (Universal imaging).

Histological Analysis—Hearts from mice were extirpated and fixed by paraformaldehyde. The fixed hearts were embedded and sectioned (3 μm thickness). The heart sections were stained with hematoxylin and eosin (H&E), Masson's trichrome, or picrosirius red. The digital images for the stained sections were taken by a Biozero microscope (BZ-8000, Keyence). The degree of fibrosis in the images was estimated by BZ-analyzer (BZ-9000, Keyence).

Real Time RT-PCR—Total RNA was extracted from mouse hearts using RNeasy fibrous tissue kit (Qiagen) according to the

manufacturer's instructions. Real time RT-PCR was performed as described previously by TaqMan RT-PCR (26). The results were normalized to 18 S RNA or *Gapdh*. Sequences for PCR primers and TaqMan probes were described in a previous report (26).

Echocardiographic and Hemodynamic Measurement—Left ventricular functions were assessed by transthoracic echocardiography. Recordings were performed using Nemio GX image analyzing system (SSA-580A, Toshiba Medical Systems). Under anesthesia, a micromanometer and conductance 1.4F catheter (SPR-671, Millar Instruments) was inserted into left ventricle. After stabilization, the signals were recorded. The signals were analyzed by Digi-Med Heart Performance Analyzer (Micro-Med) and Digi-Med System Integrator (Micro-Med).

Statistical Analysis—The results are presented as mean ± S.E. from at least three independent experiments. Statistical comparisons were performed with Student's *t* test (for two groups) or analysis of variance followed by Student-Newman-Keuls procedure (for multiple groups).

RESULTS

Administration of Metoprolol to Wild Type Normal Mice Induces Cardiac Fibrosis—During the analysis of the effects of β-blockers on heart failure, we found that long-term treatment with metoprolol, but not with propranolol and carvedilol, to wild type normal ddY mice induced perivascular fibrosis in their hearts (Fig. 1, *A* and *B*). The metoprolol-induced cardiac fibrosis was confirmed by quantitative mRNA analysis, which demonstrates that the expression of fibrotic genes, such as *Col1a* (encoding Collagen 1α (Col1a)) and *Ctgf* (encoding connective tissue growth factor (CTGF)) (31, 32), was increased in metoprolol-treated mice (Fig. 1*C*). Although increased fibrosis with metoprolol was observed with ddY mice, knock-out mice are not available for ddY mice. We then examined the effects of metoprolol on cardiac fibrosis in C57BL/6J mice (Fig. 1*D*) and found that metoprolol-induced cardiac fibrosis is independent of strain. We next examined whether metoprolol-induced fibrosis affects cardiac morphology and functions. Echocardiography and catheter measurements of metoprolol-treated mice revealed that ventricular wall thickness is decreased (supplemental Fig. S1). Among the parameters of the cardiac functions, one of the best indicators for defects of cardiac functions by fibrosis is dP/dt_{min} (26, 33). The value of dP/dt_{min} was significantly decreased by metoprolol treatment (Fig. 1*E*), suggesting that metoprolol-induced cardiac fibrosis is associated with a decrease in dP/dt_{min}. However, metoprolol did not induce hypertrophy.

Metoprolol-induced Fibrotic Response Was Independent of G-protein Signaling—To investigate the molecular mechanism of cardiac fibrosis with metoprolol, we first examined whether metoprolol couples with G_s or G_i. HEK293 cells stably expressing the β_1-adrenergic receptor were established, and cAMP accumulation by various β-blockers was then monitored in the presence of ICI118551, a β_2-adrenergic receptor-selective blocker. ICI118551 was included to exclude the involvement of the β_2-adrenergic receptor. In this study, cAMP accumulation was measured by a fluorescence resonance energy transfer probe, as described elsewhere (30). Fig. 2*A* shows that several β-blockers increased cAMP accumulation, but metoprolol did not. This result indicates that metoprolol does not activate G_s.

We also examined whether metoprolol activates G_i. Inclusion of a phosphodiesterase inhibitor, 3-isobutyl-1-methylxanthine, increased cAMP accumulation. Metoprolol inhibited cAMP accumulation (Fig. 2*B*), consistent with the report that metoprolol is an inverse agonist (34). The decreased cAMP accumulation by metoprolol was not affected by pertussis toxin treatment, indicating that metoprolol did not activate G_i (Fig. 2*B*). CGP-20712A is another inverse agonist and inhibited cAMP response similarly to metoprolol (35). These results demonstrate that metoprolol does not require G_s and G_i to induce a fibrotic response.

Metoprolol Induced the Expression of Fibrotic Genes in Cardiomyocytes—We examined whether metoprolol up-regulates the expression of fibrotic genes in cardiomyocytes and cardiac fibroblasts. Real time PCR experiments revealed that treatment of rat neonatal cardiomyocytes with metoprolol increased the expression of fibrotic genes, *Tgfβ* (encoding TGF-β), *Ctgf*, and *Col1a* (Fig. 3*A*). On the other hand, carvedilol stimulation did not induce expression of *Tgfβ* in rat neonatal cardiomyocytes (supplemental Fig. S2). In contrast to the results in cardiomyocytes, metoprolol did not increase the expression of fibrotic genes in cardiac fibroblasts, which mainly contribute to cardiac fibrosis (Fig. 3*B*). These results suggest that the induction of fibrotic genes by metoprolol is evoked through the β-adrenergic receptor in cardiomyocytes.

Metoprolol-induced Response through β_1-Adrenergic Receptor Depends on β-Arrestin2—Recent reports demonstrated that β-blockers activate β-adrenergic receptor-mediated and G protein-independent signaling (19–21). In several studies, G protein-independent signaling requires β-arrestins. Thus, we examined whether the induction of cardiac fibrosis by metoprolol treatment required β-arrestins. At first, we examined whether β-arrestin1/2 interacts with the β_1-adrenergic receptor using by BRET assay. The BRET assay is a powerful technique to detect the weak interaction between an activated receptor and its downstream molecules (24). The β_1-adrenergic receptor tagged with *Renilla* luciferase (*R*luc) and β-arrestin1 fused with GFP^2 or β-arrestin2 fused with GFP^2 (supplemental Fig. S3*A*) were transiently co-expressed in HEK293 cells. The metoprolol-stimulated BRET signal was then measured. Stimulation of the cells with isoproterenol, a full agonist for β-adrenergic receptors, strongly increased the BRET ratio in both cells expressing β_1-adrenergic receptor-*R*luc and GFP^2-β-arrestin1 or expressing β_1-adrenergic receptor-*R*luc and β-arrestin2-GFP^2. When metoprolol were added to the cells, the BRET ratio was increased only in cells expressing β_1-adrenergic receptor-*R*luc and β-arrestin2, although the interaction is fairly weak compared with that of isoproterenol (Fig. 4*A*). This result indicates that the β_1-adrenergic receptor interacts weakly with β-arrestin2 but not β-arrestin1 by the binding of metoprolol to the receptor. As HEK293 cells are different from cardiomyocytes in some aspects, we further performed similar experiments with cardiomyocytes and a rat heart myoblast cell line, H9c2. Isoproterenol increased the BRET ratios in H9c2 cells (Fig. 4*B*) and cardiomyocytes (Fig. 4*C*). Metoprolol also

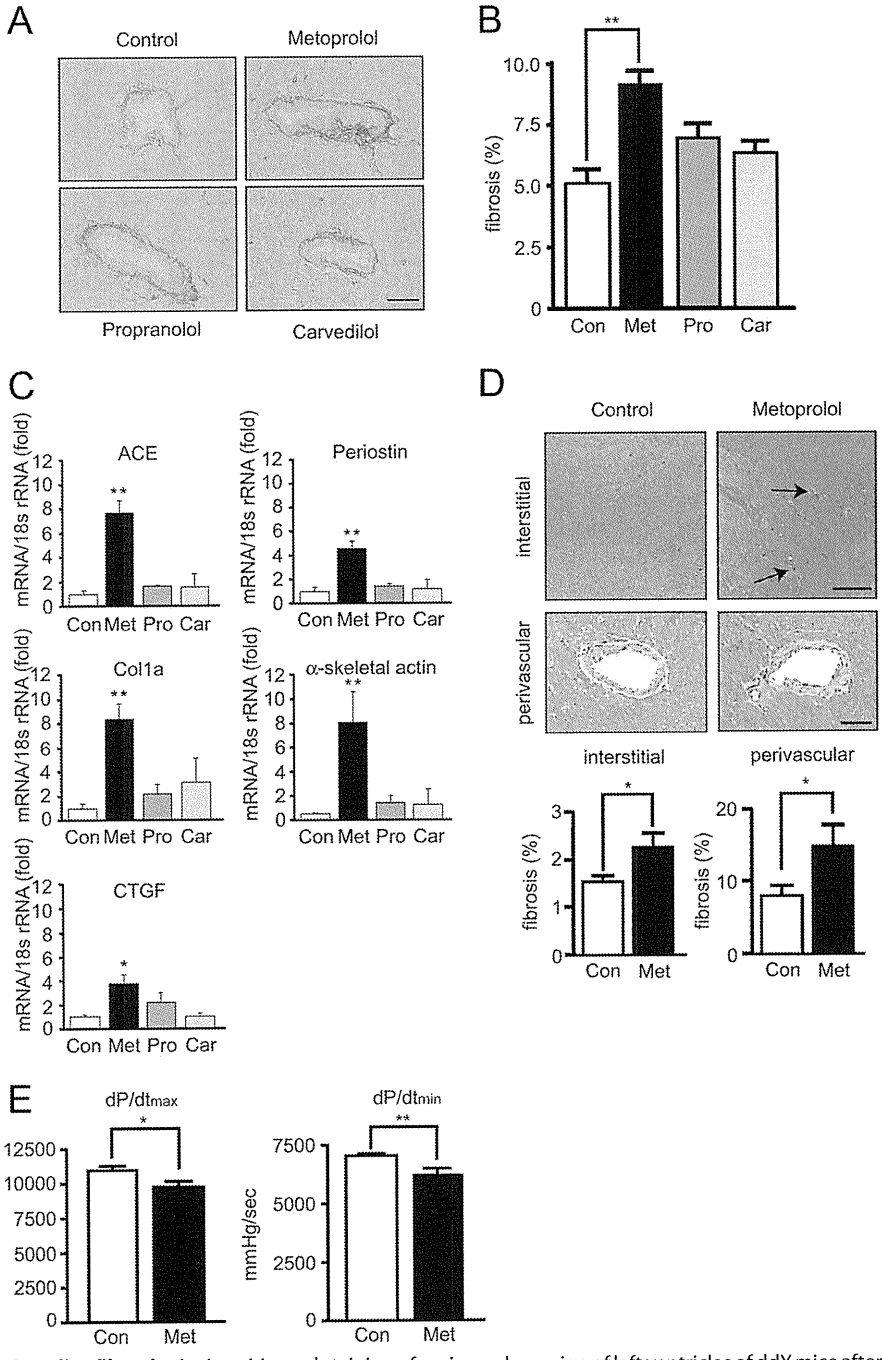

FIGURE 1. **Metoprolol-induced cardiac fibrosis.** *A*, picrosirius red staining of perivascular region of left ventricles of ddY mice after treatment of saline (*Control* (Con)) or β-blockers (Metoprolol (*Met*), Propranolol (*Pro*), Carvedilol (*Car*)). Paraffin sections of hearts (3 μm thickness) were prepared from mice, to which each β-blocker was administered. The sections were stained with picrosirius red and observed under microscopy. Representative images are shown. *Scale bar*, 15 μm. *B*, quantification of collagen volume fraction from *A* ($n = 5$). **, $p < 0.01$. *C*, up-regulation of mRNA expressions of angiotensin converting enzyme (*ACE*), Periostin, Collagen 1a (*Col1a*), α-skeletal actin, and *Ctgf* (CTGF) in mouse hearts by β-blockers. The expression levels of the fibrotic genes were evaluated by real-time RT-PCR. The fold-increases were calculated by the values of saline-treated mice set as 1 ($n = 3$–5). **, $p < 0.01$. *D*, Masson's trichrome staining of perivascular and interstitial regions of left ventricles from saline- or metoprolol-treated C57BL/6J mice ($n = 5$–6). Typical images are shown. *Arrows* indicate the fibrotic region. *Scale bar*: 15 μm on perivascular images, 30 μm on interstitial images. Collagen volume fraction on each image was quantified and the data were shown below the images. *, $p < 0.05$. *E*, hemodynamic parameters (dP/dt_{max} or dP/dt_{min}) of the saline- or metoprolol-treated C57BL/6J mice. Saline or metoprolol was administered to mice for 3 months. After the administration, they were subjected to hemodynamic measurements. The parameters dP/dt_{max} or dP/dt_{min} represent the maximal rate of pressure development, maximal rate of decay of pressure, respectively. *Error bars* show S.E. ($n = 15$). *, $p < 0.05$; **, $p < 0.01$.

increased the BRET ratios in both cells, although the extents of metoprolol-induced BRET ratios in H9c2 cells were small as compared with those in HEK293 cells. The reason of small changes in metoprolol-induced BRET ratios in H9c2 cells is unknown. As isoproterenol and metoprolol activate β-arrestin2 through the β_1-adrenergic receptor, we next examined the conformational changes of β-arrestin2 by metoprolol and isoproterenol stimulation by a BRET assay using a β-arrestin2-based biosensor, *R*luc-β-arrestin2-GFP[2] (28) (supplemental Fig. S3*B*). The biosensor was reported to detect the conforma-

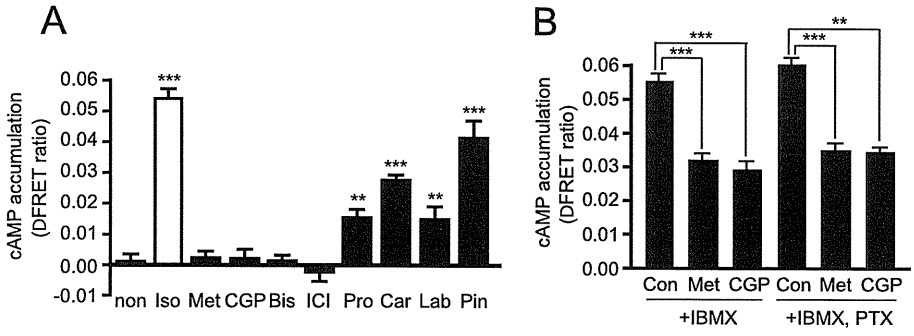

FIGURE 2. **Metoprolol-induced fibrotic responses did not depend on G protein signaling.** *A*, cAMP accumulation in HEK293 cells expressing β_1-adrenergic receptors by β-blockers (10 μM) in the presence of ICI118551 (50 μM). HEK293 cells stably expressing β_1-adrenergic receptor were transiently transfected with a FRET-based cAMP biosensor. After 15 min of pre-treatment with ICI118551, β-blocker stimulation was performed on the cells and the changes of the fluorescence were followed under microscopy. *non*, nonstimulated cell; *Iso*, isopreterenol; *Met*, metoprolol; *CGP*, CGP20712A; *Bis*, bisoprolol; *ICI*, ICI18,551; *Pro*, propranolol; *Car*, carvedilol; *Lab*, labetalol; *Pin*, pindolol. ΔFRET ratios were determined at 5 min after the stimulation. The experiments were repeated three times and each result was obtained from 13 to 20 cells. **, $p < 0.01$; ***, $p < 0.001$. *B*, pertussis toxin (*PTX*) treatment did not influence cAMP accumulation by metoprolol. PTX treatment (100 ng/ml) was performed 16 h before the co-addition of 3-isobutyl-1-methyxanthine (*IBMX*) (1 mM) and β-blockers (Metoprolol, CGP-20712A) (10 μM) on HEK293 cells stably expressing β_1-adrenergic receptor, and cAMP accumulation was determined by FRET using microscopy. The experiments were repeated three times and each result was obtained from 6 cells.

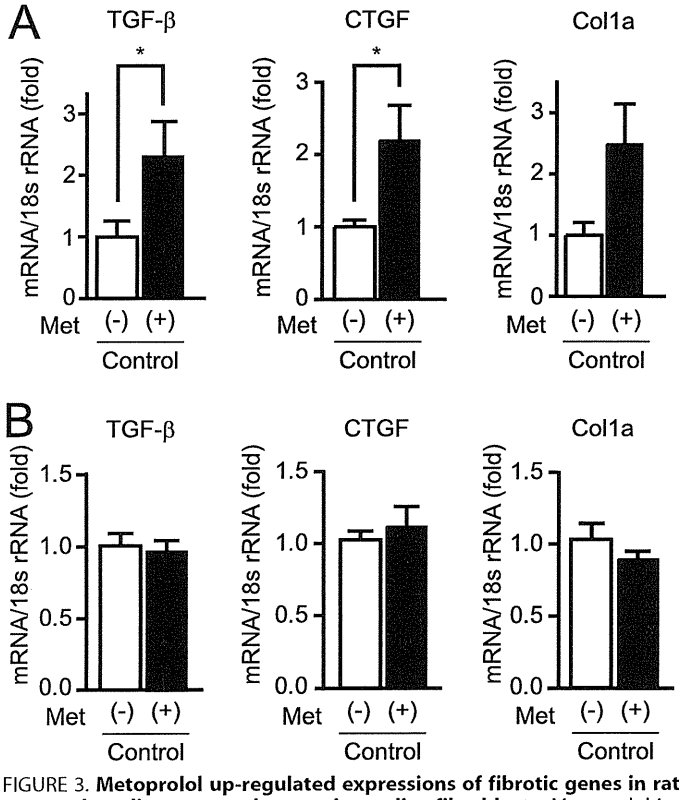

FIGURE 3. **Metoprolol up-regulated expressions of fibrotic genes in rat neonatal cardiomyocytes but not in cardiac fibroblasts.** Metoprolol-induced induction of fibrotic genes in rat neonatal cardiomyocytes (*A*) or cardiac fibroblasts (*B*) were determined ($n = 3$ for cardiomyocytes, and $n = 8$ for cardiac fibroblast). Rat neonatal cardiomyocytes or cardiac fibroblasts were stimulated with 10 μM metoprolol. The expression levels of fibrotic genes (*TGF-β*, *Ctgf* (CTGF), and *Col1a* (Col1a)) after the stimulation were determined by real time RT-PCR. *, $p < 0.05$.

tional changes of β-arrestin2 caused by both G protein-dependent and -independent pathways through GPCRs such as the angiotensin II receptor (28, 36). As shown in Fig. 4, *D* and *E*, the BRET ratios were increased by isoproterenol stimulation of HEK293 cells expressing the β_1-adrenergic receptor and H9c2 cells expressing the β_1-adrenergic receptor. In contrast, metoprolol stimulation decreased it, indicating that conformation of β-arrestin2 by metoprolol stimulation was different from that by isoproterenol stimulation (Fig. 4, *D* and *E*).

Metoprolol-induced Fibrosis in Mice Hearts Depends on β-Arrestin2—Next, we examined whether β-arrestin2 is required for metoprolol-induced cardiac fibrosis *in vivo*. Metoprolol was orally administered to β-arrestin2-KO mice twice a day for 3 months. Cardiac functions and fibrosis were then examined. Metoprolol treatment induced fibrosis in the perivascular and interstitial regions of wild type but not β-arrestin2-KO hearts (Fig. 5, *A* and *B*). Up-regulation of a fibrotic gene, *Ctgf*, with metoprolol was inhibited in β-arrestin2-KO mice (Fig. 5*C*). Consistent with these results, metoprolol-induced impairment of cardiac function was not observed in β-arrestin2-KO mice (Fig. 5*D*). These results demonstrate that β-arrestin2 is essential for metoprolol-induced cardiac fibrosis.

Metoprolol-induced Fibrosis in Mice Hearts Depends on GRK5—As GRK5 and GRK6 are often involved in a G protein-independent and β-arrestin2-dependent pathway (20, 22, 23, 36, 37), we examined their potential involvement in metoprolol-induced cardiac fibrosis. At first, we knocked down GRK5 or GRK6 in HEK293 cells (supplemental Fig. S4, *A* and *B*) and measured the interaction between the β_1-adrenergic receptor and β-arrestin2 with the BRET assay. Knockdown of GRK5 but not GRK6 inhibited the metoprolol-stimulated interaction of the β_1-adrenergic receptor with β-arrestin2 (Fig. 6*A*). Metoprolol was next administered to GRK5- or GRK6-KO mice. Cardiac dysfunction reflected by a decrease of dP/dt_{min} was observed in wild type and GRK6-KO mice, but not in GRK5-KO mice (Fig. 6*B*). Metoprolol-induced cardiac fibrosis (Fig. 6, *C* and *D*) was not evoked in β-arrestin2-KO and GRK5-KO mice. These results demonstrate that GRK5 but not GRK6 is required for metoprolol-induced cardiac fibrosis.

DISCUSSION

In this study, we demonstrated that metoprolol is a biased ligand and could induce cardiac fibrosis through a G protein-independent and GRK5/β-arrestin2-dependent pathway (Fig. 7). Accumulating evidence has implicated that β-arrestin-mediated biased signaling is elicited by stimulation of various seven-transmembrane receptors with their corresponding agonists (11, 22–25). However, there are only a few reports that the physiological meaning of this biased signaling are clearly dem-

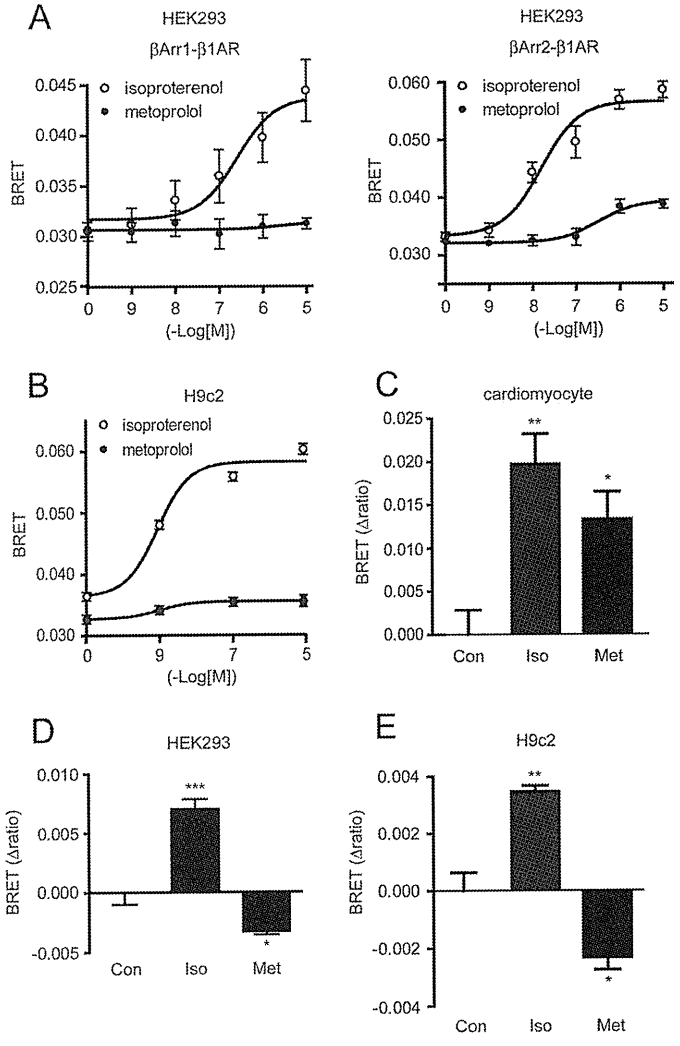

FIGURE 4. **Requirement of β-arrestin2 for metoprolol-induced responses.** *A–C*, the changes in BRET ratios by metoprolol or isoproterenol stimulation for 5 min in HEK293 cells (*A*), H9c2 cells (*B*), or cardiomyocytes (*C*). *A*, HEK293 cells were transfected with β_1-adrenergic receptor-*R*luc and GFP^2-β-arrestin1 (*left panel*, βArr1-β_1AR) or β_1-adrenergic receptor-*R*luc and β-arrestin2-GFP^2 (*right panel*, βArr2-β_1AR) ($n = 4$). *B* and *C*, H9c2 cells (*B*) or rat neonatal cardiomyocytes (*C*) were transfected with β_1-adrenergic receptor-*R*luc and β-arrestin2-GFP^2 ($n = 3$). They were harvested 48 h after the transfection, washed with PBS, and split into 96-well plates. Then, they were incubated with isoproterenol or metoprolol at the indicated concentrations for 5 min. After the incubation, *R*luc substrate, DeepBlueC™ was added to a final concentration of 5 μM. BRET signal was determined by calculating the ratio of the light emitted by the GFP^2 and the light emitted by *R*Luc. *D* and *E*, the cells were transfected with *R*luc-β-arrestin2-GFP^2 ($n = 4$ for HEK293 cells and $n = 3$ for H9c2 cells). Then, the changes in BRET ratios of *R*luc-β-arrestin2-GFP^2 were determined after metoprolol (10 μM) or isoproterenol stimulation (10 μM) for 5 min in HEK293 cells expressing β_1-adrenergic receptor (*D*) or H9c2 cells expressing β_1-adrenergic receptor (*E*). *, $p < 0.05$; **, $p < 0.01$; ***, $p < 0.001$.

onstrated *in vivo* (36, 38). In addition to those agonists, it has been shown that some β-blockers also trigger the β-arrestin-mediated biased signaling. Among β-blockers, carvedilol (21, 39) and alprenolol (20) have been reported to activate intracellular signaling in HEK293 cells through the β_2- and β_1-adrenergic receptors in a β-arrestin-dependent manner. The β-arrestin-mediated signaling by alprenolol and carvedilol transactivates the EGF receptor, resulting in ERK activation. However, how such a pathway by two β-blockers is related with physiological or pathological responses still remains to be determined. In this study, we revealed that the G protein-independent and β-arrestin2-dependent pathway evoked by a β-blocker could influence physiological responses, cardiac fibrosis, and impairment of diastolic function. The β-arrestin-mediated biased signaling by metoprolol did not induce EGF receptor transactivation (supplemental Movies S1 and S2). Thus, the β-arrestin-mediated biased pathway seemed to be different from that by carvedilol and alprenolol.

Metoprolol increased the expression of fibrotic genes in cardiomyocytes but not cardiac fibroblasts *in vitro* (Fig. 3). This result is consistent with previous reports that metoprolol is a β_1-adrenergic receptor-selective antagonist (40) and cardiac fibroblasts express only β_2-adrenergic receptor subtype (41). Metoprolol also induced the interaction of β_1-adrenergic receptor with β-arrestin2 in different cell types, such as HEK293 cells, H9c2 cells, and cardiomyocytes. From these results, we propose that metoprolol directly acts on β_1-adrenergic receptors expressed on cardiomyocytes *in vivo*. This would induce the release of the fibrotic factors from cardiomyocytes, resulting in the activation of cardiac fibroblasts to induce fibrosis.

GRK5 but not GRK6 is required for the G protein-independent and β-arrestin2-dependent cardiac fibrosis by metoprolol. Among GRK family proteins, GRK5 and GRK6 were reported to be involved in seven-transmembrane receptor-mediated biased signaling that is independent of G protein signaling and dependent on β-arrestins (22, 23, 36, 37). In these reports, the roles of GRK5 and GRK6 seem to be the same and functional differences between two GRKs in the signaling have not been detected. Accordingly, the specific contribution of GRK5 to cardiac fibrosis induced by metoprolol is unique in G protein-independent and β-arrestin-dependent signaling. For agonist-promoted desensitization, the different sets of Ser or Thr on a given GPCR undergo cell- and tissue-specific phosphorylation by different kinases in a barcode-like fashion (42–44). It was recently reported that CCL21 is a natural biased agonsit for CCR7, a seven-transmembrane chemokine receptor, and the ligand recruits β-arrestin2 only by GRK6-promoted phosphorylation of the receptor (45). Our results, together with their report, suggest that different patterns of GPCR phosphorylation by GRK5 and GRK6 determine the downstream signaling through β-arrestins. Specific interaction of β_1-adrenergic receptor with β-arrestin2, but not β-arrestin1 by metoprolol stimulation also supports this hypothesis.

Our BRET assay using *R*luc-β-arrestin2-GFP^2 demonstrated that conformation of β-arrestin2 by metoprolol stimulation was different from that by isoproterenol stimulation. Recent progress with the structural analysis of GPCRs has revealed that GPCRs can form several conformations by ligand binding. The neutral antagonist, the agonist, and the inverse agonist for the β_2-adrenergic receptor induced its different conformational states (46). In addition, two distinct conformations were observed in different antagonist-bound β_1-adrenergic receptors (47). Thus, metoprolol may induce a specific conformation of the β_1-adrenergic receptor to activate the GRK5/β-arrestin2-dependent signaling pathway.

Metoprolol is used as one of the β-blockers for the treatment of various heart diseases and its effectiveness has been verified

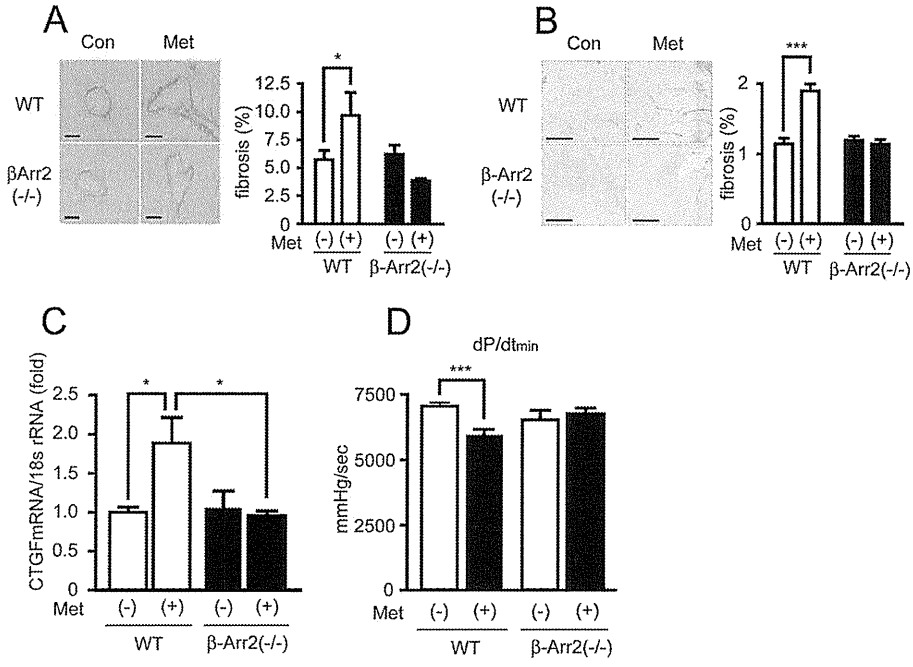

FIGURE 5. **Requirement of β-arrestin2 for metoprolol-induced cardiac fibrosis.** *A* and *B*, cardiac fibrosis in perivascular (*A*) or interstitial (*B*) regions of left ventricles of wild type or β-arrestin2-KO mice by metoprolol. Metoprolol was orally administered to wild type or β-arrestin2-KO mice for 3 months. The degrees of their cardiac fibrosis were evaluated by picrosirius staining using paraffin sections of their hearts. *, $p < 0.05$; ***, $p < 0.001$. *C*, CTGF mRNA expression by metoprolol in wild type or β-arrestin2-KO mice. *, $p < 0.05$. Mouse heart total RNA was prepared from wild-type or β-arrestin2 knock-out mice ($n = 3$), which underwent metoprolol administration for 3 months. CTGF expression levels were evaluated by real time RT-PCR. *D*, determination of dP/dt_{min} of wild type or β-arrestin2-KO mice. The metoprolol-administered wild type or β-arrestin2-KO mice were subjected to hemodynamic measurements ($n = 7$–12). ***, $p < 0.001$.

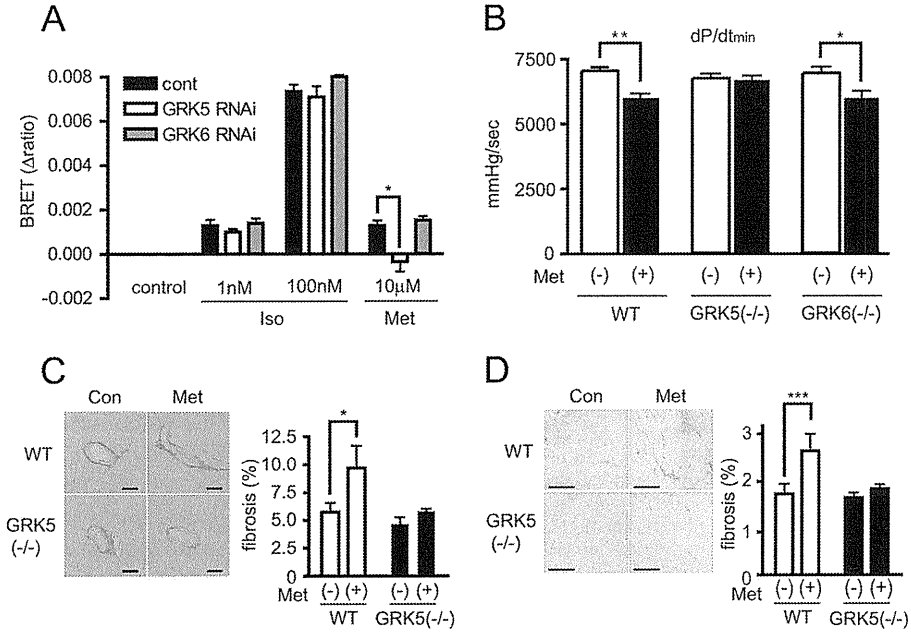

FIGURE 6. **Requirement of GRK5 for metoprolol-induced cardiac fibrosis.** *A*, interaction between β_1-adrenergic receptor and β-arrestin2 by metoprolol (10 μM) or isoproterenol (1 nM, 100 nM) stimulation in GRK5- or GRK6-knockdown cells ($n = 4$). HEK293 cells were transiently co-transfected with siRNA (control siRNA, GRK5 siRNA, or GRK6 siRNA), β_1-adrenergic receptor-*R*luc, and β-arrestin2-GFP[2]. Two days after transfection, BRET measurement was performed. *, $p < 0.05$. *B*, the changes of dP/dt_{min} in GRK5- or GRK6-KO mice ($n = 7$–14). Metoprolol was administered to wild type, GRK5-KO, or GRK6-KO mice for 3 months. After the administration, they were subjected to hemodynamic measurements. *, $p < 0.05$; **, $p < 0.01$. *C* and *D*, cardiac fibrosis in perivascular (*C*) or interstitial (*D*) regions of left ventricles of metoprolol-treated wild type or GRK5-KO mice ($n = 5$). The degrees of cardiac fibrosis in metoprolol-administered wild type or GRK5-KO mice were evaluated by picrosirius staining using paraffin sections of their hearts. *, $p < 0.05$; ***, $p < 0.001$.

by several clinical tests (48, 49). In this study, we demonstrated that long-term administration of metoprolol induced cardiac fibrosis and impaired diastolic function. Although metoprolol induced cardiac fibrosis, we think that metoprolol still has a beneficial effect on the treatment of heart failure patients. The hearts of heart failure patients are overstimulated by catecholamine, and metoprolol blocks the action of catecholamine. The degree of metoprolol-induced fibrosis is fairly small when

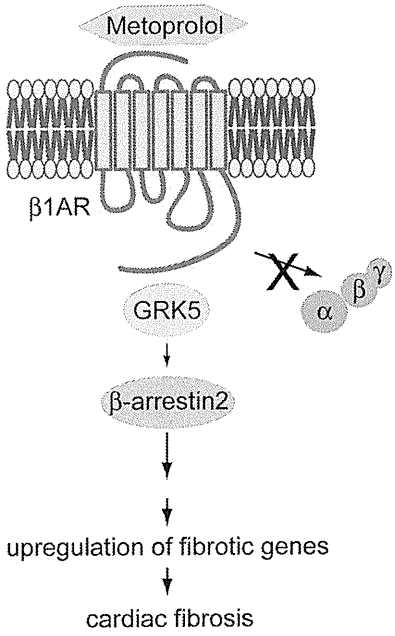

FIGURE 7. **Schematic diagram depicting the model of metoprolol-mediated cardiac fibrosis.** Metoprolol induces cardiac fibrosis through β_1-adrenergic receptor depending on GRK5 and β-arrestin2.

compared with the fibrosis induced by heart failure. Accordingly, a small increase in fibrosis by metoprolol will be overcome by the beneficial effects of the β-blocking action of metoprolol. However, it is interesting to compare the effects of metoprolol to those of carvedilol and other β-blockers on the treatment of the patients who have not suffered from fibrosis to examine the role of β-blocker-induced fibrosis.

It was recently reported that β-blockers affect calcium signaling through β-arrestin2-biased signaling in central nervous system neurons (39). It was suggested that this β-arrestin2-biased signaling explains some of the adverse effects of β-blockers on central nervous system functions. So far, β-blockers are classified by affinity, subtype selectivity, duration of action and so on (50). In this study, we focused on metoprolol in the activation of β-arrestin2-mediated biased signaling and the induction of cardiac fibrosis. This study, and studies from other groups, will help to establish that β-arrestin2-dependent signaling is another index for classifying β-blockers (20, 21, 39).

Acknowledgments—We thank Dr. R. J. Lefkowitz (Duke University) for β-arrestin2-KO mice and Dr. R. T. Premont (Duke University) for GRK5- and GRK6-KO mice. We appreciate the technical support from the Research Support Center, Graduate School of Medical Sciences, Kyushu University.

REFERENCES

1. Pierce, K. L., Premont, R. T., and Lefkowitz, R. J. (2002) Seven-transmembrane receptors. *Nat. Rev. Mol. Cell Biol.* **3,** 639–650
2. Reiter, E., and Lefkowitz, R. J. (2006) GRKs and β-arrestins. Roles in receptor silencing, trafficking, and signaling. *Trends Endocrinol. Metab.* **17,** 159–165
3. DeFea, K. A. (2011) β-Arrestins as regulators of signal termination and transduction. How do they determine what to scaffold? *Cell. Signal.* **23,** 621–629
4. DeWire, S. M., Ahn, S., Lefkowitz, R. J., and Shenoy, S. K. (2007) β-Arrestins and cell signaling. *Annu. Rev. Physiol.* **69,** 483–510
5. Premont, R. T., and Gainetdinov, R. R. (2007) Physiological roles of G protein-coupled receptor kinases and arrestins. *Annu. Rev. Physiol.* **69,** 511–534
6. Moore, C. A., Milano, S. K., and Benovic, J. L. (2007) Regulation of receptor trafficking by GRKs and arrestins. *Annu. Rev. Physiol.* **69,** 451–482
7. Hanyaloglu, A. C., and von Zastrow, M. (2008) Regulation of GPCRs by endocytic membrane trafficking and its potential implications. *Annu. Rev. Pharmacol. Toxicol.* **48,** 537–568
8. Shenoy, S. K., McDonald, P. H., Kohout, T. A., and Lefkowitz, R. J. (2001) Regulation of receptor fate by ubiquitination of activated β_2-adrenergic receptor and β-arrestin. *Science* **294,** 1307–1313
9. Cao, T. T., Deacon, H. W., Reczek, D., Bretscher, A., and von Zastrow, M. (1999) A kinase-regulated PDZ-domain interaction controls endocytic sorting of the β_2-adrenergic receptor. *Nature* **401,** 286–290
10. Ribas, C., Penela, P., Murga, C., Salcedo, A., Garcíia-Hoz, C., Jurado-Pueyo, M., Aymerich, I., and Mayor, F., Jr. (2007) The G protein-coupled receptor kinase (GRK) interactome. Role of GRKs in GPCR regulation and signaling. *Biochim. Biophys. Acta* **1768,** 913–922
11. Rajagopal, S., Rajagopal, K., and Lefkowitz, R. J. (2010) Teaching old receptors new tricks. Biasing seven-transmembrane receptors. *Nat. Rev. Drug. Discov.* **9,** 373–386
12. Rockman, H. A., Koch, W. J., and Lefkowitz, R. J. (2002) Seven-transmembrane-spanning receptors and heart function. *Nature* **415,** 206–212
13. Brodde, O. E. (1993) β-Adrenoceptors in cardiac disease. *Pharmacol. Ther.* **60,** 405–430
14. Metra, M., Cas, L. D., di Lenarda, A., and Poole-Wilson, P. (2004) β-Blockers in heart failure. Are pharmacological differences clinically important? *Heart Fail. Rev.* **9,** 123–130
15. Leimbach, W. N., Jr., Wallin, B. G., Victor, R. G., Aylward, P. E., Sundlöf, G., and Mark, A. L. (1986) Direct evidence from intraneural recordings for increased central sympathetic outflow in patients with heart failure. *Circulation* **73,** 913–919
16. Thomas, J. A., and Marks, B. H. (1978) Plasma norepinephrine in congestive heart failure. *Am. J. Cardiol.* **41,** 233–243
17. Bristow, M. R. (2000) β-Adrenergic receptor blockade in chronic heart failure. *Circulation* **101,** 558–569
18. Cruickshank, J. M. (2007) Are we misunderstanding β-blockers. *Int. J. Cardiol.* **120,** 10–27
19. Azzi, M., Charest, P. G., Angers, S., Rousseau, G., Kohout, T., Bouvier, M., and Piñeyro, G. (2003) β-Arrestin-mediated activation of MAPK by inverse agonists reveals distinct active conformations for G protein-coupled receptors. *Proc. Natl. Acad. Sci. U.S.A.* **100,** 11406–11411
20. Kim, I. M., Tilley, D. G., Chen, J., Salazar, N. C., Whalen, E. J., Violin, J. D., and Rockman, H. A. (2008) β-Blockers alprenolol and carvedilol stimulate β-arrestin-mediated EGFR transactivation. *Proc. Natl. Acad. Sci. U.S.A.* **105,** 14555–14560
21. Wisler, J. W., DeWire, S. M., Whalen, E. J., Violin, J. D., Drake, M. T., Ahn, S., Shenoy, S. K., and Lefkowitz, R. J. (2007) A unique mechanism of β-blocker action. Carvedilol stimulates β-arrestin signaling. *Proc. Natl. Acad. Sci. U.S.A.* **104,** 16657–16662
22. Kim, J., Ahn, S., Ren, X. R., Whalen, E. J., Reiter, E., Wei, H., and Lefkowitz, R. J. (2005) Functional antagonism of different G protein-coupled receptor kinases for β-arrestin-mediated angiotensin II receptor signaling. *Proc. Natl. Acad. Sci. U.S.A.* **102,** 1442–1447
23. Ren, X. R., Reiter, E., Ahn, S., Kim, J., Chen, W., and Lefkowitz, R. J. (2005) Different G protein-coupled receptor kinases govern G protein and β-arrestin-mediated signaling of V2 vasopressin receptor. *Proc. Natl. Acad. Sci. U.S.A.* **102,** 1448–1453
24. Shukla, A. K., Violin, J. D., Whalen, E. J., Gesty-Palmer, D., Shenoy, S. K., and Lefkowitz, R. J. (2008) Distinct conformational changes in β-arrestin report biased agonism at seven-transmembrane receptors. *Proc. Natl. Acad. Sci. U.S.A.* **105,** 9988–9993
25. Wei, H., Ahn, S., Shenoy, S. K., Karnik, S. S., Hunyady, L., Luttrell, L. M., and Lefkowitz, R. J. (2003) Independent β-arrestin 2 and G protein-mediated pathways for angiotensin II activation of extracellular signal-regulated kinases 1 and 2. *Proc. Natl. Acad. Sci. U.S.A.* **100,** 10782–10787
26. Nishida, M., Sato, Y., Uemura, A., Narita, Y., Tozaki-Saitoh, H., Nakaya,

M., Ide, T., Suzuki, K., Inoue, K., Nagao, T., and Kurose, H. (2008) P2Y6 receptor-G$\alpha_{12/13}$ signalling in cardiomyocytes triggers pressure overload-induced cardiac fibrosis. *EMBO J.* **27,** 3104–3115
27. Fujii, T., Onohara, N., Maruyama, Y., Tanabe, S., Kobayashi, H., Fukutomi, M., Nagamatsu, Y., Nishihara, N., Inoue, R., Sumimoto, H., Shibasaki, F., Nagao, T., Nishida, M., and Kurose, H. (2005) G$\alpha_{12/13}$-mediated production of reactive oxygen species is critical for angiotensin receptor-induced NFAT activation in cardiac fibroblasts. *J. Biol. Chem.* **280,** 23041–23047
28. Charest, P. G., Terrillon, S., and Bouvier, M. (2005) Monitoring agonist-promoted conformational changes of β-arrestin in living cells by intramolecular BRET. *EMBO Rep.* **6,** 334–340
29. Mangmool, S., Haga, T., Kobayashi, H., Kim, K. M., Nakata, H., Nishida, M., and Kurose, H. (2006) Clathrin required for phosphorylation and internalization of β_2-adrenergic receptor by G protein-coupled receptor kinase 2 (GRK2). *J. Biol. Chem.* **281,** 31940–31949
30. Nikolaev, V. O., Bünemann, M., Schmitteckert, E., Lohse, M. J., and Engelhardt, S. (2006) Cyclic AMP imaging in adult cardiac myocytes reveals far-reaching β_1-adrenergic but locally confined β_2-adrenergic receptor-mediated signaling. *Circ. Res.* **99,** 1084–1091
31. Daniels, A., van Bilsen, M., Goldschmeding, R., van der Vusse, G. J., and van Nieuwenhoven, F. A. (2009) Connective tissue growth factor and cardiac fibrosis. *Acta Physiol.* **195,** 321–338
32. Ruiz-Ortega, M., Rodríguez-Vita, J., Sanchez-Lopez, E., Carvajal, G., and Egido, J. (2007) TGF-β signaling in vascular fibrosis. *Cardiovasc. Res.* **74,** 196–206
33. Yamamoto, K., Masuyama, T., Sakata, Y., Nishikawa, N., Mano, T., Yoshida, J., Miwa, T., Sugawara, M., Yamaguchi, Y., Ookawara, T., Suzuki, K., and Hori, M. (2002) Myocardial stiffness is determined by ventricular fibrosis, but not by compensatory or excessive hypertrophy in hypertensive heart. *Cardiovasc. Res.* **55,** 76–82
34. Varma, D. R., Shen, H., Deng, X. F., Peri, K. G., Chemtob, S., and Mulay, S. (1999) Inverse agonist activities of β-adrenoceptor antagonists in rat myocardium. *Br. J. Pharmacol.* **127,** 895–902
35. Engelhardt, S., Grimmer, Y., Fan, G. H., and Lohse, M. J. (2001) Constitutive activity of the human β_1-adrenergic receptor in β_1-receptor transgenic mice. *Mol. Pharmacol.* **60,** 712–717
36. Rakesh, K., Yoo, B., Kim, I. M., Salazar, N., Kim, K. S., and Rockman, H. A. (2010) β-Arrestin-biased agonism of the angiotensin receptor induced by mechanical stress. *Sci. Signal.* **3,** ra46
37. Noma, T., Lemaire, A., Naga Prasad, S. V., Barki-Harrington, L., Tilley, D. G., Chen, J., Le Corvoisier, P., Violin, J. D., Wei, H., Lefkowitz, R. J., and Rockman, H. A. (2007) β-Arrestin-mediated β_1-adrenergic receptor transactivation of the EGFR confers cardioprotection. *J. Clin. Invest.* **117,** 2445–2458
38. Gesty-Palmer, D., Flannery, P., Yuan, L., Corsino, L., Spurney, R., Lefkowitz, R. J., and Luttrell, L. M. (2009) A β-arrestin-biased agonist of the parathyroid hormone receptor (PTH1R) promotes bone formation independent of G protein activation. *Sci. Transl. Med.* **1,** 1ra1
39. Tzingounis, A. V., von Zastrow, M., and Yudowski, G. A. (2010) β-Blocker drugs mediate calcium signaling in native central nervous system neurons by β-arrestin-biased agonism. *Proc. Natl. Acad. Sci. U.S.A.* **107,** 21028–21033
40. Bristow, M. R. (2011) Treatment of chronic heart failure with β-adrenergic receptor antagonists. A convergence of receptor pharmacology and clinical cardiology. *Circ. Res.* **109,** 1176–1194
41. Gustafsson, A. B., Brunton, L. L. (2000) β-Adrenergic stimulation of rat cardiac fibroblasts enhances induction of nitric-oxide synthase by interleukin-1β via message stabilization. *Mol. Pharmacol.* **58,** 1470–1478
42. Butcher, A. J., Prihandoko, R., Kong, K. C., McWilliams, P., Edwards, J. M., Bottrill, A., Mistry, S., and Tobin, A. B. (2011) Differential G protein-coupled receptor phosphorylation provides evidence for a signaling bar code. *J. Biol. Chem.* **286,** 11506–11518
43. Torrecilla, I., Spragg, E. J., Poulin, B., McWilliams, P. J., Mistry, S. C., Blaukat, A., and Tobin, A. B. (2007) Phosphorylation and regulation of a G protein-coupled receptor by protein kinase CK2. *J. Cell Biol.* **177,** 127–137
44. Nobles, K. N., Xiao, K., Ahn, S., Shukla, A. K., Lam, C. M., Rajagopal, S., Strachan, R. T., Huang, T. Y., Bressler, E. A., Hara, M. R., Shenoy, S. K., Gygi, S. P., and Lefkowitz, R. J. (2011) Distinct phosphorylation sites on the β_2-adrenergic receptor establish a barcode that encodes differential functions of β-arrestin. *Sci. Signal.* **4,** ra51
45. Zidar, D. A., Violin, J. D., Whalen, E. J., and Lefkowitz, R. J. (2009) Selective engagement of G protein-coupled receptor kinases (GRKs) encodes distinct functions of biased ligands. *Proc. Natl. Acad. Sci. U.S.A.* **106,** 9649–9654
46. Bokoch, M. P., Zou, Y., Rasmussen, S. G., Liu, C. W., Nygaard, R., Rosenbaum, D. M., Fung, J. J., Choi, H. J., Thian, F. S., Kobilka, T. S., Puglisi, J. D., Weis, W. I., Pardo, L., Prosser, R. S., Mueller, L., and Kobilka, B. K. (2010) Ligand-specific regulation of the extracellular surface of a G protein-coupled receptor. *Nature* **463,** 108–112
47. Moukhametzianov, R., Warne, T., Edwards, P. C., Serrano-Vega, M. J., Leslie, A. G., Tate, C. G., and Schertler, G. F. (2011) Two distinct conformations of helix 6 observed in antagonist-bound structures of a β_1-adrenergic receptor. *Proc. Natl. Acad. Sci. U.S.A.* **108,** 8228–8232
48. Group, M. H. S. (1999) Effect of metoprolol CR/XL in chronic heart failure. Metoprolol CR/XL randomized intervention trial in congestive heart failure (MERIT-HF). *Lancet* **353,** 2001–2007
49. Waagstein, F., Caidahl, K., Wallentin, I., Bergh, C. H., and Hjalmarson, A. (1989) Long-term β-blockade in dilated cardiomyopathy. Effects of short- and long-term metoprolol treatment followed by withdrawal and readministration of metoprolol. *Circulation* **80,** 551–563
50. Reiter, M. J. (2004) Cardiovascular drug class specificity, β-blockers. *Prog. Cardiovasc. Dis.* **47,** 11–33

Supplemental Information

Supplemental method

Time-Lapse imaging of EGFR internalization

The coding region of human EGF receptor (EGFR) was fused to EGFP at its C-terminus and was subcloned into pcDNA3 vector. The HEK293cells were transfected with EGFR-EGFP on 35 mm glass-base dishes (IWAKI). Two days after transfection, the medium was replaced by serum-free DMEM/F12 medium without phenol red (Invitrogen) for microscopic observation. The cells were observed for 15 min under Olympus *IX81* Motorized Inverted *Microscope* equipped with a cooled charge-coupled device camera (Cool SNAP HQ; Roper Scientific) and then, treated with ICI118551 to exclude the involvement of β_2-adrenergic receptor. Fifteen min after the treatment, β-blockers were added to the cells. The images for DIC and GFP were taken every 3 min. The images were analyzed by MetaMorph software.

Supplemental Figure S1 Changes of cardiac geometry by long-term administration of metoprolol. (A) Two representative M-mode Echocardiographic images are shown. The quantitative analysis of the Heart Rate (HR) (B), end-diastolic interventricular septum thickness (IVSTd) (C), left ventricular end-diastolic internal diameter (LVIDd) (D), ejection fraction (EF) (E), left ventricular end-diastolic posterior wall diameter (LVPWd) (F), left ventricular end-systolic internal diameter (LVIDs) (G), fractional shortening (FS) (H) are presented. (N=15) **, $P<0.01$; ***, $P<0.001$.

Supplemental Figure S2 Carvedilol did not increase the expression of TGF-β in rat neonatal cardiomyocytes. Rat neonatal cardiomyocytes were stimulated with 10 μM carvedilol. The results were normalized to GAPDH. The fold increase was calculated by the value of cells with DMSO treatment (con) set as 1. Error bars indicate SEM (N=10). n.s., not significant

Supplemental Figure S3 Schematic images of the probes used in BRET experiments. (a) Intermolecular BRET using β_1-adrenergic receptor (β_1-AR) tagged with *Renilla* luciferase (Rluc) and β-arrestin2 fused with GFP^2. β_1-AR-Rluc co-expressed with β-arrestin2-GFP^2 undergoes BRET upon ligand binding to the receptor. (b) Intramolecular BRET using RLuc-β-arrestin2-GFP^2 to measure conformational changes in β-arrestin2 by receptor stimulation. The distance between Rluc and GFP^2 depends on the conformational changes of β-arrestin2 by various stimulations. BRET ratio increases when Rluc comes close to GFP^2, while BRET ratio decreases when Rluc becomes distant from

GFP^2.

Supplemental Figure S4 Effects of GRK5/6 siRNAs on the expression of GRK5/6 mRNAs. RNA was extracted from HEK293 cells treated with GRK5 siRNA or GRK6 siRNA. Expression level of GRK5 or GRK6 was analyzed by qRT-PCR. (a) Quantification of GRK5 expression level (normalized to GAPDH) (N=4). (b) Quantification of GRK6 expression level (normalized to GAPDH). Error bars indicate SEM (N=4). **, $P<0.01$.

Supplemental Movie S1 Time-lapse imaging videos of EGFR internalization after carvedilol stimulation on HEK293 cells. Scale bar, 20 μm

Supplemental Movie S2 Time-lapse imaging videos of EGFR internalization after metoprolol stimulation on HEK293 cells. Scale bar, 20 μm

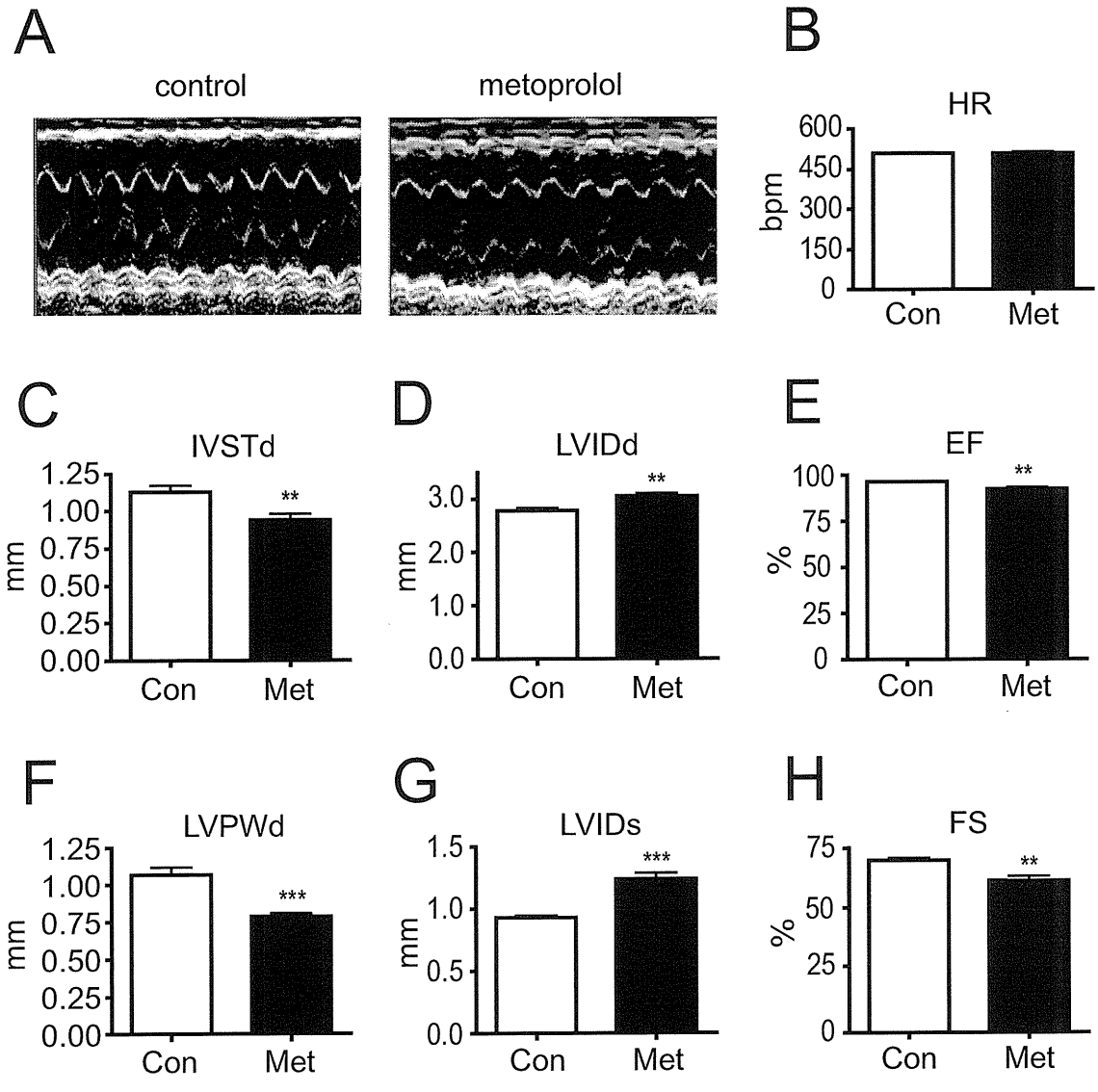

Supplemental Figure 1

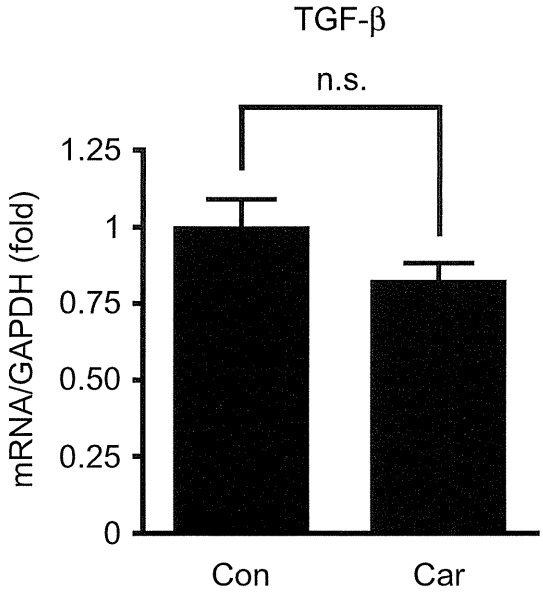

Supplemental Figure 2

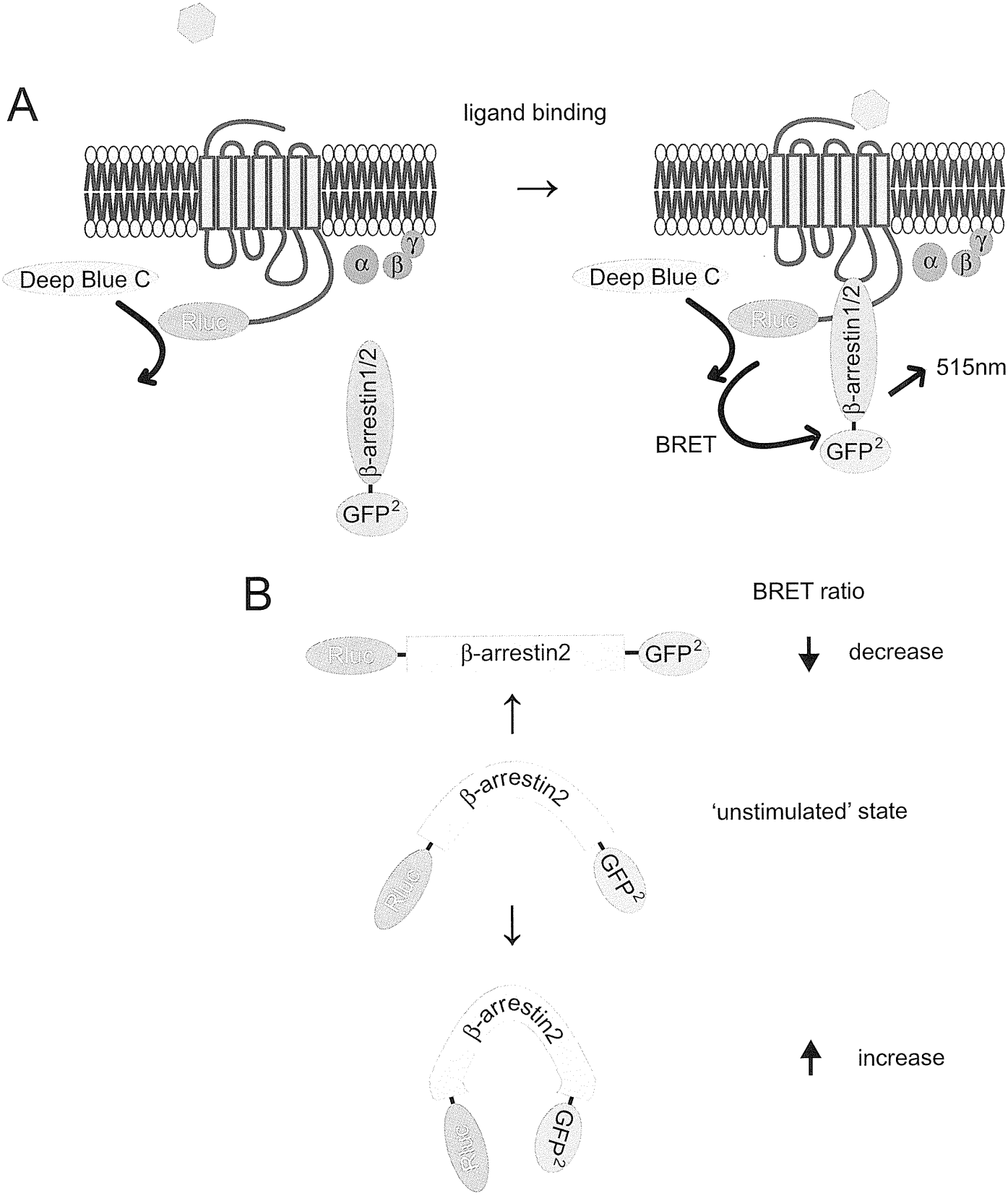

Supplemental Figure 3

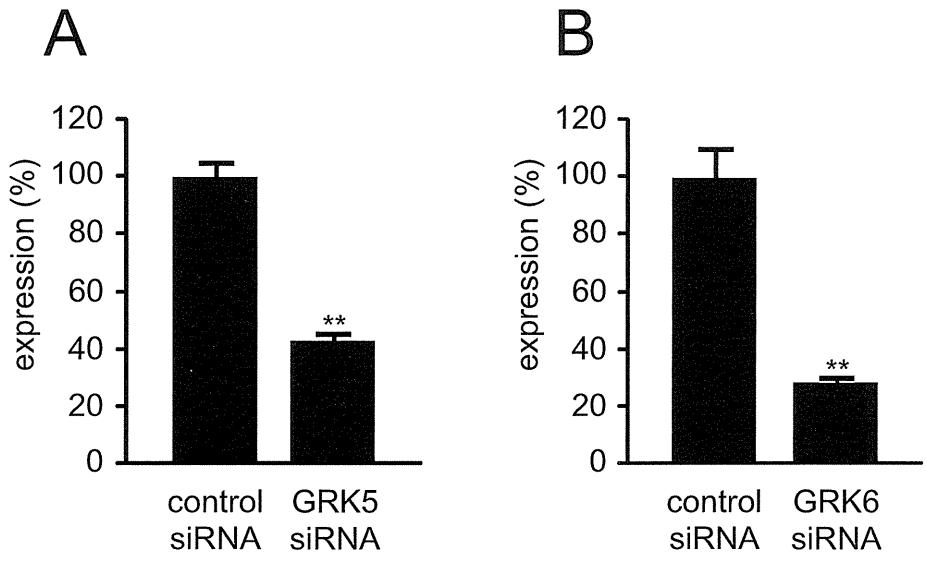

Supplemental Figure 4

OPEN ACCESS Freely available online

PLoS one

Highly Sensitive In Vitro Methods for Detection of Residual Undifferentiated Cells in Retinal Pigment Epithelial Cells Derived from Human iPS Cells

Takuya Kuroda[1,2], Satoshi Yasuda[1], Shinji Kusakawa[1,2], Naoya Hirata[3], Yasunari Kanda[3], Kazuhiro Suzuki[1], Masayo Takahashi[2,4], Shin-Ichi Nishikawa[2,5], Shin Kawamata[2], Yoji Sato[1,2,6]*

1 Division of Cellular and Gene Therapy Products, National Institute of Health Sciences, Tokyo, Japan, **2** Foundation for Biomedical Research and Innovation, Kobe, Japan, **3** Division of Pharmacology, National Institute of Health Sciences, Tokyo, Japan, **4** Laboratory for Retinal Regeneration, RIKEN Center for Developmental Biology, Kobe, Japan, **5** Laboratory of Stem Cell Research, RIKEN Center for Developmental Biology, Kobe, Japan, **6** Department of Pharmaceutical Quality Science, Graduate School of Pharmaceutical Sciences, Nagoya City University, Nagoya, Japan

Abstract

Human induced pluripotent stem cells (hiPSCs) possess the capabilities of self-renewal and differentiation into multiple cell types, and they are free of the ethical problems associated with human embryonic stem cells (hESCs). These characteristics make hiPSCs a promising choice for future regenerative medicine research. There are significant obstacles, however, preventing the clinical use of hiPSCs. One of the most obvious safety issues is the presence of residual undifferentiated cells that have tumorigenic potential. To locate residual undifferentiated cells, in vivo teratoma formation assays have been performed with immunodeficient animals, which is both costly and time-consuming. Here, we examined three in vitro assay methods to detect undifferentiated cells (designated an in vitro tumorigenicity assay): soft agar colony formation assay, flow cytometry assay and quantitative real-time polymerase chain reaction assay (qRT-PCR). Although the soft agar colony formation assay was unable to detect hiPSCs even in the presence of a ROCK inhibitor that permits survival of dissociated hiPSCs/hESCs, the flow cytometry assay using anti-TRA-1-60 antibody detected 0.1% undifferentiated hiPSCs that were spiked in primary retinal pigment epithelial (RPE) cells. Moreover, qRT-PCR with a specific probe and primers was found to detect a trace amount of Lin28 mRNA, which is equivalent to that present in a mixture of a single hiPSC and 5.0×10^4 RPE cells. Our findings provide highly sensitive and quantitative in vitro assays essential for facilitating safety profiling of hiPSC-derived products for future regenerative medicine research.

Citation: Kuroda T, Yasuda S, Kusakawa S, Hirata N, Kanda Y, et al. (2012) Highly Sensitive In Vitro Methods for Detection of Residual Undifferentiated Cells in Retinal Pigment Epithelial Cells Derived from Human iPS Cells. PLoS ONE 7(5): e37342. doi:10.1371/journal.pone.0037342

Editor: Edward Chaum, University of Tennessee, United States of America

Received January 23, 2012; **Accepted** April 20, 2012; **Published** May 17, 2012

Funding: This work was supported by a Strategic Fund for the Promotion of Science and Technology from Japan Science and Technology Agency, and Research Grants H21-SAISEI-IPPAN-021, H23-SAISEI-IPPAN-004&005 and H23-IYAKU-IPPAN-001 from the Japanese Ministry of Health, Labour and Welfare. The funders had no role in study design, data collection and analysis, decision to publish, or preparation of the manuscript.

Competing Interests: The authors have declared that no competing interests exist.

* E-mail: yoji@nihs.go.jp

Introduction

Pluripotent stem cells such as embryonic stem cells and induced pluripotent stem cells have two capabilities: 1) pluripotency: the ability to differentiate into a variety of cells and 2) self-renewal: the ability to undergo numerous cycles of cell division while maintaining their cellular identity. Because of these two characteristics, it has been expected that they would provide new sources for robust and continuous production of a variety of cells and tissues for regenerative medicine/cell therapy. Additionally, hiPSCs offer us a possible solution to the ethical problems and the immune rejection of hESC-derived cells, thus raising novel avenues for patient-specific cell therapy. As previously reported [1,2], many attempts are currently underway to differentiate hESCs and hiPSCs into various tissues: cardiomyocytes [2,3], neurons [2,4], and hepatocytes [5,6]. It is noteworthy that clinical trials have been conducted with retinal pigment epithelial (RPE) cells derived from hESCs to treat patients with dry age-related macular degeneration and Stargardt's macular dystrophy by Advanced Cell Technology. hiPSCs have also been shown to differentiate into RPE cells, which display functionality both *in vitro* and *in vivo* [7,8]. Thus, autologous transplant of hiPSC-derived RPE cells holds great promise in the clinical therapy of macular degeneration.

Although hiPSCs overcome immunogenic and ethical barriers, the translation of hiPSCs into the clinical setting faces the same significant problems as those of hESCs. One of the most important issues in the development of a safe pharmaceutical or medical device derived from human pluripotent stem cells is ensuring that the final product does not form tumors after implantation [9]. There are two primary concerns. First, the cell-based product may be unstable and transform to produce a tumor, which is a common problem for any cell-based products, regardless of the cell types of the raw materials. Second, the product derived from human pluripotent stem cells might contain residual undifferentiated stem cells that would eventually proliferate and form a teratoma [10]. Previous reports have shown that several hundred hESCs were sufficient for generating tumors in immunodeficient mice [11,12]. Hence, to adress the second concern above, it is critical to develop

highly sensitive assays for detection of residual undifferentiated stem cells in the final products, and to determine their lower limit of detection (LLOD). An evaluation study of the *in vivo* tumorigenicity assay using severe combined immunodeficiency (SCID) mice has shown that 245 undifferentiated hESCs spiked into 10^6 feeder fibroblasts produce a teratoma [11]. On the other hand, some *in vitro* assays, such as quantitative real-time polymerase chain reaction (qRT-PCR), flow cytometry and immunohistochemistry, have been used to indicate the undifferentiated state of stem cells with various markers (such as Oct-3/4, Nanog, Sox2, TRA-1-60, TRA-1-81, SSEA-3 and SSEA-4) [13–15]. However, it has not been determined how many residual undifferentiated hiPSCs can be detected by these *in vitro* assays.

In this study, to establish a high sensitivity assay for detection of residual undifferentiated hiPSCs in the final product, we evaluated three *in vitro* assays: soft agar colony formation assay, flow cytometry and qRT-PCR. To achieve this goal, these assays were used on cell mixtures that contained defined numbers of undifferentiated hiPSCs in primary RPE cells, and we also tried to determine the LLOD of each assay by using multiple lots of primary RPE cells as backgrounds. Through this process, we revealed that one-step qRT-PCR using probes and primers targeting Lin28 transcripts can detect levels as low as 0.002% residual undifferentiated cells in hiPSC-derived RPE cells.

Results

In vitro differentiation of hiPSCs into retinal pigment epithelial cells

Minimizing contamination of undifferentiated pluripotent stem cells in cell therapy products is crucial because of the risk of tumorigenesis. To evaluate residual undifferentiated hiPSCs in differentiated cells, it is necessary to determine the LLOD of the hiPSC content in RPE cells. First, we differentiated hiPSCs into RPE cells using the *in vitro* differentiation protocol previously described (Fig. 1A) [7]. The hiPSC-derived RPE cells exhibited polygonal, cobblestone-like morphology, an indication of RPE maturation, which is similar to that of the primary RPE cells (Fig. 1B). Immunocytochemical staining revealed that N-cadherin, the major cadherin expressed in RPE cells [16], showed a distribution to the tight junction of the hiPSC-derived RPE cells, which is consistent with primary RPE cells (Fig. 1C). Moreover, in flow cytometry experiments, a strong expression of the visual cycle protein CRALBP and the melanosomal matrix protein GP-100 was detected in both primary RPE and hiPSC-derived RPE cells compared to in undifferentiated hiPSCs (Fig. 1D). To characterize developmental stages during RPE differentiation, a qRT-PCR assay was used to identify transcript levels of CRALBP and the visual cycle protein RPE65, indicating that CRALBP and RPE65 increased as differentiation progresses and were equally well expressed both in the mature hiPSC-derived RPE cells and primary RPE cells (Fig. 1E). Together, these data showed that mature RPE cells differentiated from hiPSCs possess similar properties to primary RPE cells.

Soft agar colony formation assay of hiPSCs

The soft agar colony formation assay is a general method to monitor anchorage-independent growth, which is considered the most appropriate *in vitro* assay for detecting the malignant transformation of cells [17]. To measure cell transformation quantitatively, we used the CytoSelect 96-well Cell Transformation Assay, as described in the Materials and Methods section. Previous reports have shown that human pluripotent stem cells undergo apoptosis when dissociated into single cells [18]. However, preparation of single cell suspension is quite important because the presence of cell clumps or adjacent cells is critical for growth in an agar medium. Thus, we first sought to clarify whether single hiPSCs grow in the soft agar medium. The soft agar colony formation assay showed that single-hiPSCs could not proliferate in the agar medium. In addition, the ROCK inhibitor Y-27632, which has been reported to inhibit apoptosis [19], did not improve survival of hiPSCs under our conditions (Fig. 2A and S1A). These results demonstrated that the soft agar colony formation assay is not appropriate for detection of undifferentiated hiPSCs in single cell suspension.

Next, we tested whether colony formation of the human ovarian teratocarcinoma cell line PA-1 [20] occurs in an agar medium, since PA-1 cells could mimic possible malignant cells derived from hiPSC. PA-1 cells efficiently formed colonies in soft agar depending on the number of cells (Fig. S1B). On the other hand, primary RPE cells did not grow in a soft agar media with 1.0×10^4 cells/well, even when cultured for 30 days (Fig. S1C). Based on these results, we aimed to examine the sensitivity of the soft agar colony formation assay to detect PA-1 cells. We spiked 100 (1%), 50 (0.5%), and 25 (0.25%) PA-1 cells into 1×10^4 primary RPE cells in order to define the minimum number of PA-1 cells required to grow in a soft agar media. The largest number of PA-1 cells (1%) gave rise to detectable colonies within 20 days, whereas lesser numbers of PA-1 cells (0.5% and 0.25%) required 30 days until the colonies become detectable (Fig. 2A and B). We next tried to determine the LLOD of the soft agar colony formation assay. The LLOD of the assay signal was calculated as the mean plus 3.3 fold the standard deviation of the measurement of negative controls [21]. Based on signals from three lots of primary RPE cells as a negative control (1.71 ± 0.40 [fold over the background signal]), the LLOD of the soft agar transformation assay was calculated as 3.03 (Fig. 2C). These results indicate that at least 1% spiked PA-1 cells are necessary for detecting colonies in primary RPE cells using the soft agar transformation assay (4.4 ± 1.1). As shown in Fig. 2C, the hiPSC-derived RPE cells showed no colony formation in the soft agar medium, and the assay signal was lower than the LLOD (1.21 ± 0.19). These results suggest that the contamination of transformed cells, assuming that their anchorage independency is comparable to PA-1, is less than 1% in the hiPSC-derived RPE cells.

Detection of undifferentiated hiPSCs by flow cytometry

In the second set of the experiments, we tried to detect residual undifferentiated cells via flow cytometry. Using five antibodies which recognize stem cell marker antigens (Oct3/4, Nanog, Sox2, TRA-1-60, TRA-1-81), we first attempted to identify highly selective markers that distinguish a small population of hiPSCs from primary RPE cells. To minimize nonspecific staining, we used fluorescent conjugated monoclonal antibodies for the flow cytometry. All of the stem cell markers were detected in undifferentiated hiPSCs, but the levels of cell staining differed between the antibodies, presumably attributable to the protein expression in the cells and/or the avidity of the antibodies. The fluorescence histograms of hiPSCs and primary RPE cells showed that anti-Oct3/4, anti-Sox2 and anti-TRA-1-60 antibodies clearly distinguished hiPSCs from RPE cells (Fig. 3A). Because TRA1-60 is not only a marker of undifferentiated hiPSCs but also of embryonal carcinoma [22], we employed anti-TRA-1-60 antibody in further experiments. The TRA-1-60$^+$ gate was defined as including at most 0.05% of the primary RPE cells with the highest fluorescence (Fig. 3B). In the flow cytometry, the mean and standard deviation of TRA-1-60$^+$ cells in the primary RPE cells (the negative controls) were 26.6 and 15.6 cells/10^5 cells,

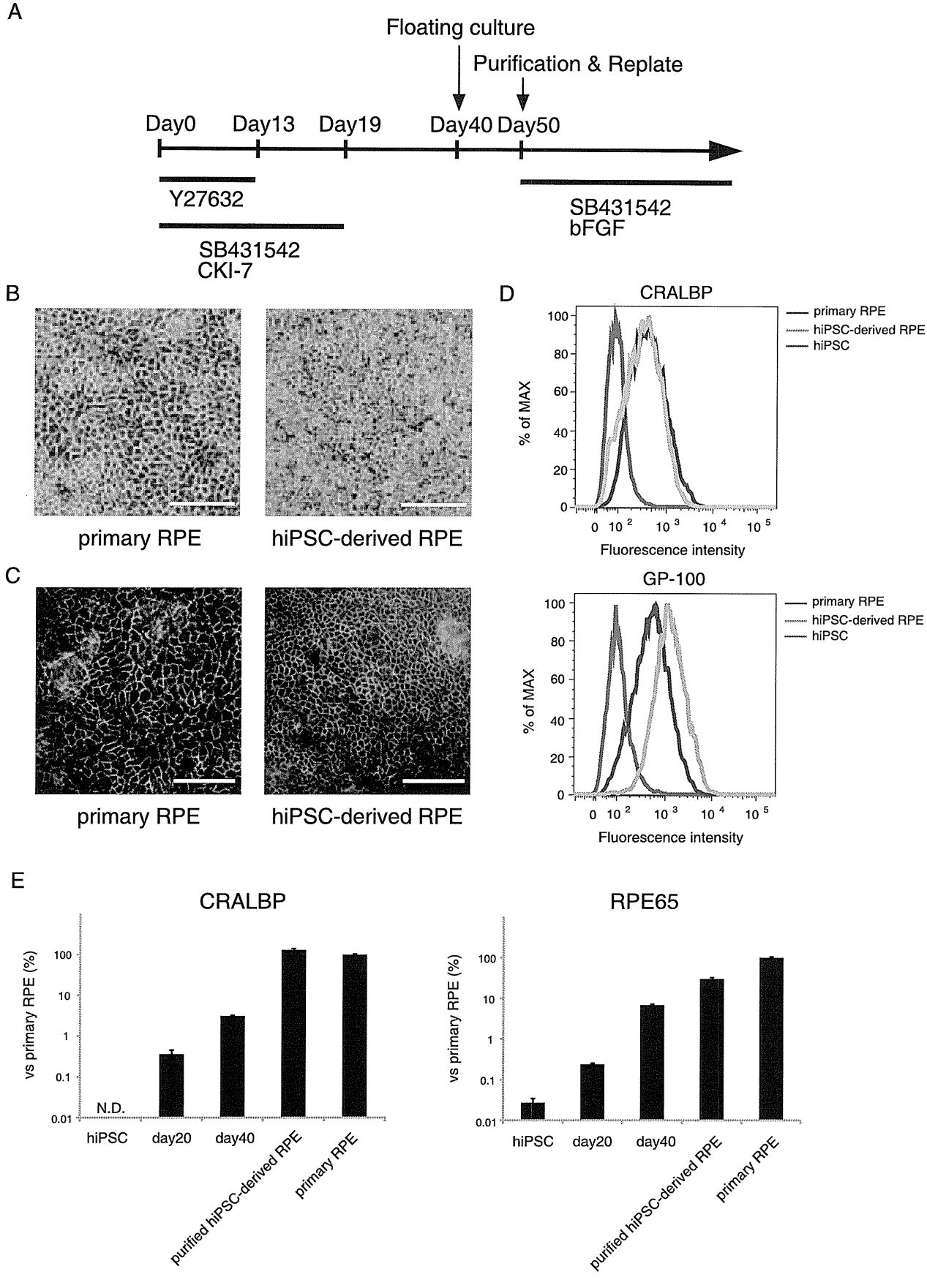
A
Floating culture
Purification & Replate
Day0
Day13
Day19
Day40
Day50
Y27632
SB431542
CKI-7
SB431542
bFGF
B
primary RPE
hiPSC-derived RPE
C
primary RPE
hiPSC-derived RPE
D
CRALBP
primary RPE
hiPSC-derived RPE
hiPSC
% of MAX
Fluorescence intensity
GP-100
primary RPE
hiPSC-derived RPE
hiPSC
% of MAX
Fluorescence intensity
E
CRALBP
vs primary RPE (%)
N.D.
hiPSC
day20
day40
purified hiPSC-derived RPE
primary RPE
RPE65
vs primary RPE (%)
hiPSC
day20
day40
purified hiPSC-derived RPE
primary RPE

Figure 1. Differentiation of hiPSCs into retinal pigment epithelial cells. (A) Schematic diagram of the culture procedure for retinal differentiation. Photomicrograph (B) and N-cadherin staining (C) shows that both primary RPE cells and hiPSC-derived RPE cells form polygonal, cobblestone-like morphology. Scale bars, 100 μm. (D) Flow cytometry analysis of CRALBP and GP-100 expression in hiPSCs (red), hiPSC-derived RPE cells (green) and primary RPE cells (blue). (E) Time-course analysis of expression of RPE cell markers, CRALBP (left) and RPE65 (right), using qRT-PCR. Error bars represent the standard deviation of the measurements (n = 3).
doi:10.1371/journal.pone.0037342.g001

respectively, producing an LLOD of 78.1 cells/10^5 cells (Fig. 3B). To analyze the performance of the system for detection of residual hiPSCs, we spiked 2.5×10^3 (0.1%) and 2.5×10^2 (0.01%) hiPSCs into 2.5×10^6 primary RPE cells and analyzed 1.0×10^5 cells via flow cytometry using anti-TRA-1-60 antibody. We also confirmed the number of the applied hiPSCs by spiking CFDA-stained hiPSCs (Fig. S2). In the experiment shown in Fig. 3C, 130 and 19 cells were identified as TRA-1-60$^+$ cells in 0.1% and 0.01% hiPSCs spiked samples, respectively. These results indicated that at least 0.1% of residual undifferentiated hiPSCs (2.5×10^3 cells out of 2.5×10^6 cells) can be detected via the flow cytomerty. Finally, to detect residual undifferentiated cells in hiPSC-derived RPE cells, we tested 1×10^5 cells and detected six TRA-1-60$^+$ cells, suggesting that the population of undifferentiated hiPSCs in the hiPSC-derived RPE cells was no more than 0.1% (Fig. 3D).

Detection of undifferentiated hiPSCs via qRT-PCR

We next tested the ability of qRT-PCRs to detect a trace amount of stem cell-specific mRNA. To identify highly selective markers for undifferentiated hiPSCs, we compared the mRNA levels of OCT3/4, KLF4, c-MYC, SOX2, NANOG, LIN28 and REX1 in hiPSCs and primary RPE cells (Fig. 4A). Primary RPE cells were found to endogenously express c-Myc at 25.49% of the levels observed in hiPSC, which was consistent with the previous finding that MEF expressed c-Myc at approximately 20% of levels observed in mouse ES cells [23]. The expression levels of Klf4 and Rex1 in primary RPE cells were 3.51% and 2.23% compared with hiPSCs, respectively. On the other hand, more than a 1000-fold difference between primary RPE cells and hiPSCs was observed in the gene expression of Nanog (0.07%), Sox2 (0.06%), Oct3/4 (0.01%) and Lin28 (not detected). These results suggested that the latter four genes are useful in detecting hiPSCs in RPE cells.

We then conducted two sets of qRT-PCR assays to evaluate the utility of these marker genes to detect spiked hiPSCs in primary RPE cells. We first measured mRNA levels of Nanog, Oct3/4 and Lin28 in the five lots of primary RPE cells (the negative control) to determine the LLOD. The LLODs for Nanog and Oct3/4 mRNAs were 0.45% and 0.04% those of hiPSCs, respectively (Fig. 4B). The LLOD of Lin28 could not be calculated because no fluorescent signal for Lin28 expression was detectable in the primary RPE cells. These results along with experiments spiking 2.5×10^4 (1%), 2.5×10^3 (0.1%) and 2.5×10^2 (0.01%) hiPSCs into 2.5×10^6 primary RPE cells (Fig. 4B) indicated that measurements of Nanog, Oct3/4 and Lin28 expression by qRT-PCRs could detect at least 1%, 0.1% and 0.01% contamination of residual undifferentiated hiPSCs in RPE cells, respectively.

Finally, we examined whether qRT-PCR for Lin28 was applicable in the detection of residual undifferentiated cells in differentiated RPE cells from hiPSCs. Total RNA (250 ng) extracted from the differentiating cells (day 5, 20, and 40) and purified hiPSC-derived RPE cells (the passage number 3 and 4) were subjected to qRT-PCR analysis. The mRNA level of Lin28 was continuously down-regulated during the differentiation process, being 0.02% that of hiPSCs at day 40. In early passage culture (passage number 3) after purification, Lin28 was still significantly expressed at a level 0.002% that of hiPSCs. From passage 4 onward, however, no detectable level of Lin28 expression was observed in hiPSC-derived RPE cells (Fig. 4C). These results suggest that qRT-PCR analysis for Lin28 detects 0.002% of residual undifferentiated hiPSCs in hiPSC-induced PRE cells, namely, that a single hiPSC in 5.0×10^4 RPE cells is detectable.

Discussion

For the clinical use of products derived from human pluripotent stem cells, it is essential to improve both the efficacy and safety of the final product. In order to develop safe hiPSC-based treatments, the hurdle of tumorigenicity arising from undifferentiated cells must be overcome [9]. To address the issue of tumorigenicity, some recent publications have advocated the development of protocols for the derivation of hiPSC [23–25] and have outlined methods for the elimination of residual hESCs [26]. However, to date, more than several hundred cells are necessary for human pluripotent stem cells to form a tumor in immunocompromised mice [11]. Therefore, highly sensitive tumorigenicity assays and their standardization are necessary for detecting a small population of residual undifferentiated cells in products derived from human pluripotent stem cells.

In the present study, we evaluated three methods for detection of residual undifferentiated hiPSCs in hiPSCs-derived differentiated cells: soft agar colony formation assay, flow cytometry and qRT-PCR. Table 1 summarizes the advantages and disadvantages of the assays associated with product tumorigenicity. The soft agar colony formation assay is known to be more sensitive in the detection of certain types of tumorigenic cells, compared to *in vivo* methods using immunocompromised mice [27]. However, we found the soft agar colony formation assay unsuitable for detecting residual undifferentiated hiPSCs, presumably attributable to the dissociation-induced apoptosis of hiPSCs [18]. On the other hand, flow cytometry and qRT-PCR assays were found to be able to detect a trace amount of undifferentiated cells. These two assays have been exploited for characterization of stem cell-based products, as well as undifferentiated pluripotent stem cells, but the present study is the first analytical and quantitative approach designed to evaluate the detection of residual undifferentiated cells in products derived from human pluripotent stem cells. The advantage of the flow cytometry assay is that it is able to identify undifferentiated cells. Unfortunately, the results are greatly affected by gating, and only the cells expressing the marker protein are detectable. On the other hand, the advantages of qRT-PCR are its rapidity, quantitativity and high sensitivity, whereas its disadvantage is that only the cells expressing the marker gene are detectable. Although the *in vivo* tumorigenicity assay is costly and time-consuming, it can directly analyze tumor formation in a specific microenvironment where the product is implanted (eg. retina). Therefore, a combination of relevant *in vitro* and *in vivo* assays would be necessary to ensure the safety of a product derived from human pluripotent stem cells. The rationale for the choice of specific assays would be justified, based on their characteristics shown in Table 1.

We have demonstrated that the qRT-PCR assay can successfully detect 0.002% residual undifferentiated hiPSCs in hiPSC-induced RPE cells using Lin28 as a target gene (Fig. 4E). To the best of our knowledge, this qRT-PCR assay, using solely 250 ng of

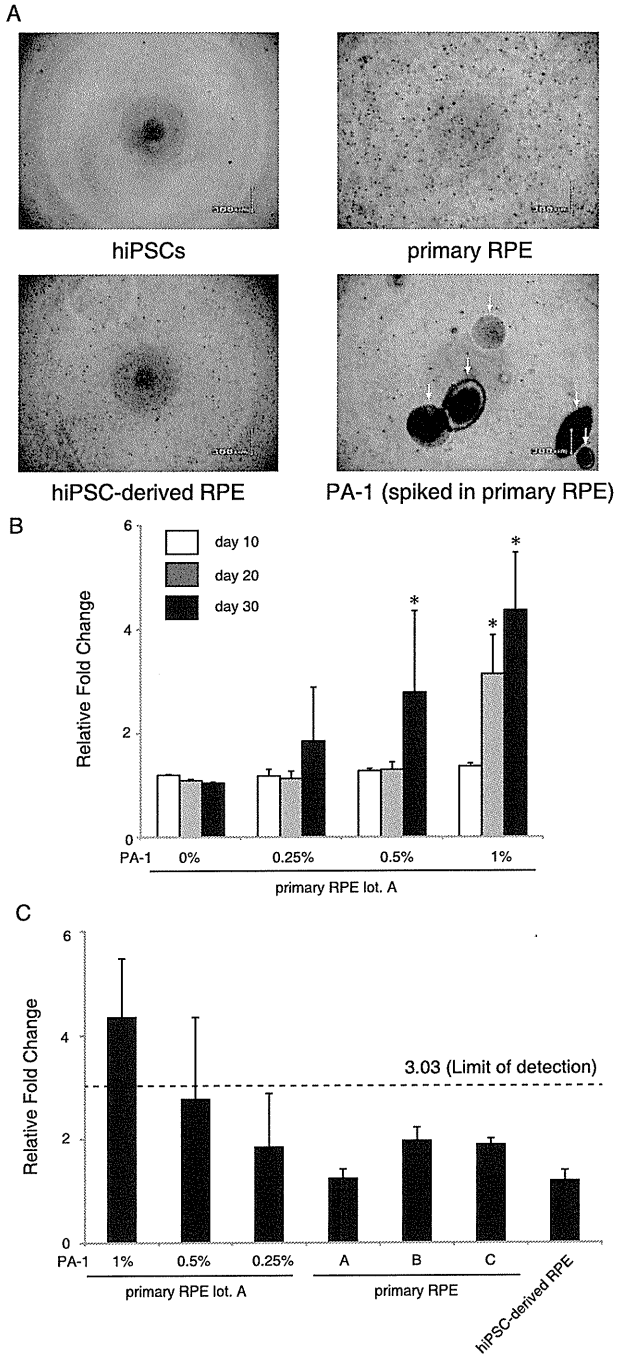

Figure 2. Soft agar colony formation assay of hiPSCs and teratocarcinoma PA-1 cells. (A) Phase-contrast images of hiPSCs, primary RPE cells, hiPSC-derived RPE cells and PA-1cells spiked into primary RPE cells (1%) cultured in soft agar medium for 30 days. Arrows indicate the colonies of PA-1 cells. (B) PA-1 cells (1%, 100 cells; 0.5%, 50 cells; 0.25%, 25 cells; 0%, 0 cells) were spiked into 1.0×10^4 primary RPE cells and grown in soft agar for 10, 20 and 30 days. Cell growth was quantified using a CytoSelect kit. Results were expressed as a relative fold change of the value of blank well. Statistical significance was determined using two-way ANOVA and Bonferroni's post-hoc test (*$P<0.05$ compared with the 0% control). (C) HiPSC-derived RPE cells, three lots of primary RPE cells and PA-1 cells spiked into primary RPE cells were grown in soft agar for 30 days. Quantification of the results is described in (B). Limit of detection was calculated as the mean plus 3.3 fold the standard deviation of the measurement of the three lots of primary RPE cells. Error bars represent the standard deviation of the measurements (n = 3).
doi:10.1371/journal.pone.0037342.g002

total RNA obtained from approximately 5×10^4 cells, is the most sensitive of the previously reported methods in detecting undifferentiated pluripotent stem cells. Lin28 is known to specifically inhibit the processing of let-7 miRNAs, which are involved in cell-fate decisions [28]. Interestingly, the aberrant expression of Lin28 transcripts has been recently reported in human germ-cell tumors [29], suggesting that Lin28 is a useful marker of germ-cell malignancy as well as of pluripotency of hiPSCs. Lin28 mRNA gradually decreased in the differentiation process and was completely diminished by passage 4 (Fig. 4C). These observations suggest that Lin28 transcripts are also available for presenting degree of differentiation in hiPSC-derived products because detection of residual Lin28 confirms the contamination of undifferentiated cells even at a late stage of differentiation. Needless to say, the distinct expression of Lin28 could possibly be observed in other normal somatic cells. However, Lin28 is, at least in part, one of the potent markers for detecting incompletely differentiated cells contained in RPE cells derived from pluripotent stem cells.

A great deal of international research is currently being directed at developing regenerative medicine using pluripotent stem cells. Until now, however, little attention has been paid to developing methods to detect undifferentiated cells in pluripotent stem cell-based products. Here, we have revealed that a qRT-PCR method targeting Lin28 can effectively detect a trace amount of hiPSCs in hiPSC-induced RPE cells and shows potential as an *in vitro* tumorigenecity assay of hiPSC-derived cells. We expect our findings to contribute to the process of validation and quality control of hiPSCs-based cell therapy products and to promote the application of regenerative medicine in the treatment of a wide variety of diseases in the near future.

Materials and Methods

Cell culture

HiPSC line 201B7 induced by transducing Oct3/4, Sox2, Klf4 and c-Myc [2] was obtained from the RIKEN Cell Bank. Undifferentiated hiPSCs were maintained on mitomycin C-treated SNL cells (a mouse fibroblast STO cell line expressing the neomycin-resistance gene cassette and LIF) in human ES cell culture medium (ReproCell, Japan) supplemented with 4 ng/ml human basic fibroblast growth factor (bFGF; WAKO, Japan). Undifferentiated colonies were passaged as small clumps once in every 5–6 days using CTK solution (ReproCell) and STEMPRO EZPassage (Invitrogen, Carlsbad, CA). Human primary RPE cells were obtained from the Lonza and ScienCell Research Laboratories. The primary RPE cells were maintained in Retinal Pigment Epithelial Cell Basal Medium (Lonza Biologics, Basel, Switzerland) containing supplements (L-glutamine, GA-1000 and bFGF; Lonza). PA-1 cells derived from human ovarian teratocarcinoma (ATCC, Manassas, VA) were maintained on Minimum Essential Medium Eagle medium (Sigma–Aldrich, St. Louis) supplemented with 10% (v/v) fetal bovine serum (FBS; Gibco, Paisley, UK). All cell lines and differentiated cells were grown in a humidified atmosphere of 5% CO_2 and 95% air at 37°C.

RPE cell differentiation of hiPSCs

The procedure for differentiating hiPSCs into RPE cells was performed according to the previously described protocol [7] as shown in Figure 1A. The hiPSC clumps were first incubated on